Published May 20, 2013

Lymphoid tissue phospholipase A_2 group IID resolves contact hypersensitivity by driving antiinflammatory lipid mediators

Yoshimi Miki,[1,2] Kei Yamamoto,[1] Yoshitaka Taketomi,[1,2] Hiroyasu Sato,[1,2] Kanako Shimo,[1,3] Tetsuyuki Kobayashi,[3] Yukio Ishikawa,[4] Toshiharu Ishii,[4] Hiroki Nakanishi,[5] Kazutaka Ikeda,[6] Ryo Taguchi,[7] Kenji Kabashima,[8] Makoto Arita,[9,10] Hiroyuki Arai,[9] Gérard Lambeau,[11] James M. Bollinger,[12,13] Shuntaro Hara,[2] Michael H. Gelb,[12,13] and Makoto Murakami[1,10]

[1]Lipid Metabolism Project, Tokyo Metropolitan Institute of Medical Science, Tokyo 156-8506, Japan
[2]Department of Health Chemistry, School of Pharmacy, Showa University, Tokyo 142-8555, Japan
[3]Department of Biology, Faculty of Science, Ochanomizu University, Tokyo112-8610, Japan
[4]Department of Pathology, Toho University School of Medicine, Tokyo 143-8540, Japan
[5]Department of Medical Biology, Akita University Graduate School of Medicine, Akita 010-8502, Japan
[6]Institute for Advanced Biosciences, Keio University, Yamagata 997-0017, Japan
[7]Department of Biomedical Sciences, College of Life and Health Sciences, Chubu University, Aichi 487-8501, Japan
[8]Department of Dermatology, Kyoto University Graduate School of Medicine, Kyoto 606-8501, Japan
[9]Department of Health Chemistry, Graduate School of Pharmaceutical Sciences, University of Tokyo, Tokyo 113-0033, Japan
[10]PRESTO, Japan Science and Technology Agency, Saitama 332-0012, Japan
[11]Institut de Pharmacologie Moléculaire et Cellulaire, UMR7275, Centre National de la Recherche Scientifique et Université de Nice-Sophia-Antipolis, 06560 Valbonne, France
[12]Department of Chemistry and [13]Department of Biochemistry, University of Washington, Seattle, WA 98195

CORRESPONDENCE
Makoto Murakami:
murakami-mk@igakuken.or.jp

Resolution of inflammation is an active process that is mediated in part by antiinflammatory lipid mediators. Although phospholipase A_2 (PLA_2) enzymes have been implicated in the promotion of inflammation through mobilizing lipid mediators, the molecular entity of PLA_2 subtypes acting upstream of antiinflammatory lipid mediators remains unknown. Herein, we show that secreted PLA_2 group IID (PLA2G2D) is preferentially expressed in $CD11c^+$ dendritic cells (DCs) and macrophages and displays a pro-resolving function. In hapten-induced contact dermatitis, resolution, not propagation, of inflammation was compromised in skin and LNs of PLA2G2D-deficient mice (*Pla2g2d*$^{-/-}$), in which the immune balance was shifted toward a proinflammatory state over an antiinflammatory state. Bone marrow-derived DCs from *Pla2g2d*$^{-/-}$ mice were hyperactivated and elicited skin inflammation after intravenous transfer into mice. Lipidomics analysis revealed that PLA2G2D in the LNs contributed to mobilization of a pool of polyunsaturated fatty acids that could serve as precursors for antiinflammatory/pro-resolving lipid mediators such as resolvin D1 and 15-deoxy-$\Delta^{12,14}$-prostaglandin J_2, which reduced Th1 cytokine production and surface MHC class II expression in LN cells or DCs. Altogether, our results highlight PLA2G2D as a "resolving $sPLA_2$" that ameliorates inflammation through mobilizing pro-resolving lipid mediators and points to a potential use of this enzyme for treatment of inflammatory disorders.

Abbreviations used: 15d-PGJ_2, 15-deoxy-$\Delta^{12,14}$-prostaglandin J_2; AA, arachidonic acid; BMDC, BM-derived DC; CHS, contact hypersensitivity; $cPLA_2$, Ca^{2+}-dependent cytosolic PLA_2; DHA, docosahexaenoic acid; DNBS, dinitrobenzene sulfonic acid; DNFB, dinitrofluorobenzene; EPA, eicosapentaenoic acid; ESI-MS, electrospray ionization mass spectrometry; HETE, hydroxyeicosatetraenoic acid; $iPLA_2$, Ca^{2+}-independent PLA_2; LA, linoleic acid; LC, liquid chromatography; LysoPC, lysophosphatidylcholine; LysoPE, lysophosphatidylethanolamine; LysoPS, lysophosphatidylserine; PC, phosphatidylcholine; PD1, protectin D1 (10(S),17(S)-dihydroxy-4Z,7Z,11E,13Z,15E,19Z-DHA); PE, phosphatidylethanolamine; PG, phosphatidylglycerol; PGD_2, prostaglandin D_2; PGE_2, prostaglandin E_2; PLA_2, phospholipase A_2; PLA2G2D, group IID $sPLA_2$; PUFA, polyunsaturated fatty acid; RvD1, resolvin D1 (7S,8R,17S-trihydroxy-4Z,9E,11E,13Z,15E,19Z-DHA); $sPLA_2$, secreted PLA_2; T reg cell, regulatory T cell.

In many acute and chronic disorders, unresolved inflammation is a major mechanism of disease pathogenesis (Libby, 2002). Inflammation is a protective host response to foreign challenge or tissue injury that, if unopposed, could lead to loss of tissue structure and function. Many inflammatory processes have self-limiting and self-resolving systems, which are regulated by antiinflammatory or pro-resolving mediators during the course of inflammation (Serhan et al., 2008). Uncontrolled balance between pro- and

Y. Miki and K. Yamamoto contributed equally to this paper.

© 2013 Miki et al. This article is distributed under the terms of an Attribution–Noncommercial–Share Alike–No Mirror Sites license for the first six months after the publication date (see http://www.rupress.org/terms). After six months it is available under a Creative Commons License (Attribution–Noncommercial–Share Alike 3.0 Unported license, as described at http://creativecommons.org/licenses/by-nc-sa/3.0/).

The Rockefeller University Press $30.00
J. Exp. Med. 2013 Vol. 210 No. 6 1217-1234
www.jem.org/cgi/doi/10.1084/jem.20121887

Supplemental Material can be found at:
http://jem.rupress.org/content/suppl/2013/05/15/jem.20121887.DC1.html

The Journal of Experimental Medicine

Downloaded from jem.rupress.org on August 18, 2013

Published May 20, 2013

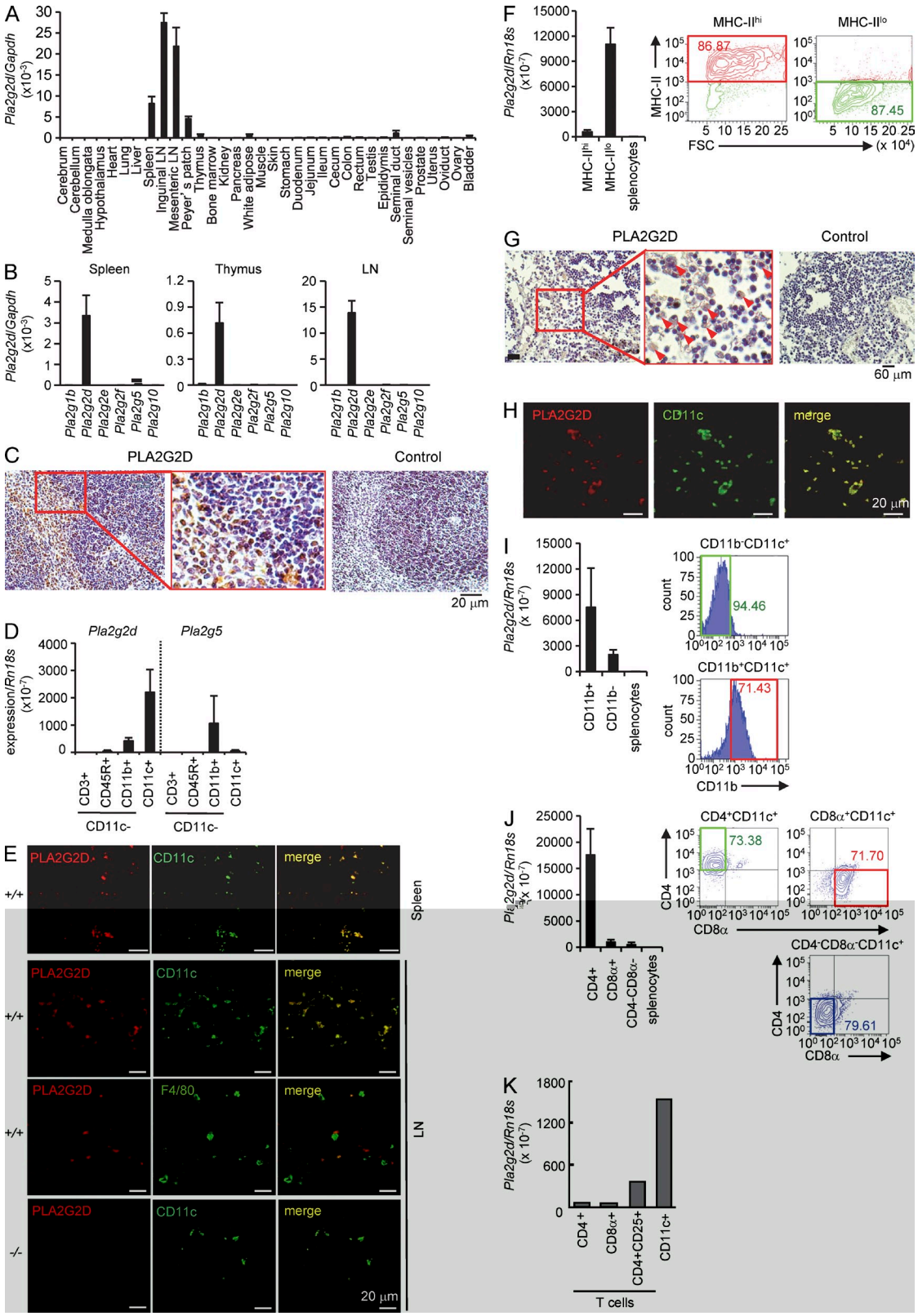

Figure 1. Expression of PLA2G2D in CD11c⁺ DCs. (A) Quantitative RT-PCR of *Pla2g2d* relative to *Gapdh* in various tissues of C57BL/6 mice (mean ± SEM from four mice, pooled from two experiments). (B) Quantitative RT-PCR of $sPLA_2$ mRNAs relative to *Gapdh* in cells from mouse spleen, thymus, and LNs (mean ± SEM from five mice, pooled from two experiments). (C) Immunohistochemistry of mouse spleen with anti–mouse PLA2G2D or control antibody. A boxed area is magnified. (D) Quantitative RT-PCR of *Pla2g2d* and *Pla2g5* relative to *Rn18s* in several splenic cell populations (mean ± SEM from

Downloaded from jem.rupress.org on August 18, 2013

Published May 20, 2013

antiinflammatory mediators is now considered to be a central feature in many cases of acute and chronic inflammation.

Lipid mediators derived from polyunsaturated fatty acids (PUFAs) have recently attracted much attention as critical regulators of inflammatory responses (Serhan, 2007). Eicosanoids, such as prostaglandins and leukotrienes derived from ω-6 arachidonic acid (AA; C20:4), are generally known as proinflammatory lipid mediators (Samuelsson et al., 1987). However, some AA metabolites such as 15-deoxy-$\Delta^{12,14}$-prostaglandin J_2 (15d-PGJ_2) and lipoxins have antiinflammatory capacities (Rossi et al., 2000; Straus et al., 2000). Furthermore, depending on tissue-specific contexts and receptor subtype occupancy, prostaglandin E_2 (PGE_2), and D_2 (PGD_2) often suppress the recruitment or activation of neutrophils, macrophages, or DCs (Gomez et al., 2005; Trivedi et al., 2006; Rajakariar et al., 2007; Honda et al., 2009). Recently, novel families of lipid mediators derived from ω-3 eicosapentaenoic acid (EPA; C20:5) and docosahexaenoic acid (DHA; C22:6), such as resolvins and protectins, have been shown to possess potent pro-resolving activities and thereby participate in the resolution of inflammation (Serhan et al., 2002; Mukherjee et al., 2004). PUFAs can also drive alternative antiinflammatory programs by acting on PUFA-sensing plasma membrane (e.g., GPR120) or nuclear (e.g., PPARγ) receptors (Diep et al., 2000; Oh et al., 2010), or by attenuating ER stress (Ariyama et al., 2010).

Biosynthesis of PUFA-derived lipid mediators is initiated by hydrolysis of phospholipids by phospholipase A_2 (PLA_2; Murakami et al., 2011). Of more than 30 members of the PLA_2 family, group IVA cytosolic $PLA_2\alpha$ ($cPLA_2\alpha$; Bonventre et al., 1997; Uozumi et al., 1997) and, in certain cases, group VIA Ca^{2+}-independent PLA_2 ($iPLA_2\beta$; Moon et al., 2008) play major roles in stimulus-coupled AA release for eicosanoid generation. However, the molecular entity of PLA_2 enzymes that can trigger antiinflammatory lipid mediator programs still remains obscure. The secreted PLA_2 ($sPLA_2$) family, which consists of 11 isoforms, has long been thought to play proinflammatory roles (Lambeau and Gelb, 2008; Murakami et al., 2010). Indeed, studies using transgenic or knockout mice for $sPLA_2$s have revealed their redundant or nonredundant proinflammatory roles in arthritis, asthma, or cardiovascular disorders through lipid mediator-dependent or -independent mechanisms (Ohtsuki et al., 2006; Bostrom et al., 2007; Henderson et al., 2007; Muñoz et al., 2007; Fujioka et al., 2008; Boilard et al., 2010). However, the simple idea that $sPLA_2$s always serve as offensive players of inflammation needs careful evaluation, as PLA2G2A protects from infection by degrading bacterial membranes (Weinrauch et al., 1996), PLA2G5 facilitates phagocytotic clearance of harmful materials by macrophages (Balestrieri et al., 2009; Boilard et al., 2010), and PLA2G10, when overexpressed in macrophages, can prime antiinflammatory, rather than proinflammatory, responses through production of PGE_2 and 15d-PGJ_2 (Curfs et al., 2008). Although $sPLA_2$s can liberate various fatty acids, including ω-3 PUFAs, in vitro, it remains unknown whether they could participate in some inflammation resolution processes by driving antiinflammatory lipid mediators in vivo.

Group IID $sPLA_2$ (PLA2G2D) was initially identified as an isoform structurally related to PLA2G2A and is abundantly expressed in lymphoid organs (Ishizaki et al., 1999; Shakhov et al., 2000; Valentin et al., 1999). Although PLA2G2D-transfected cells exhibited augmented AA release (Murakami et al., 2001) and infusion of an artificial PLA2G2D-Fc fusion protein into mice attenuated autoimmune diseases (von Allmen et al., 2009), its precise functions and mechanistic actions in vivo remain obscure. Herein, using mice lacking PLA2G2D (*Pla2g2d*$^{-/-}$), we show that PLA2G2D is a lymphoid tissue-associated "resolving $sPLA_2$" that participates in the resolution of contact hypersensitivity (CHS). This is the first demonstration of a particular $sPLA_2$ subtype that lies upstream of the pro-resolving lipid mediators in a tissue-specific context.

RESULTS

PLA2G2D is preferentially expressed in lymphoid tissue-resident DCs and macrophages

We first aimed to determine the sites where PLA2G2D is intrinsically expressed. Previous studies have reported that PLA2G2D is expressed in secondary lymphoid organs (Ishizaki et al., 1999; Valentin et al., 1999; Shakhov et al., 2000). Consistently, quantitative RT-PCR for *Pla2g2d* in various tissues of C57BL/6 mice revealed its preferential expression in secondary lymphoid organs, including inguinal and mesenteric LNs, Peyer's patch, and spleen (Fig. 1 A). Among the $sPLA_2$s, PLA2G2D is a major isoform expressed in cells from lymphoid organs (Fig. 1 B). In mouse spleen, cells with adhesive morphology and large cytoplasm in the red pulp and marginal zone, as well as focally in the white pulp, were stained with anti-PLA2G2D but not control antibody, whereas PLA2G2D staining was scarcely seen in lymphocytes (judging from round cell shape and small cytoplasm; Fig. 1 C).

three mice, a representative of three experiments). The separation procedure of individual cells is illustrated in Fig. S1. (E) Confocal immunofluorescence microscopy of PLA2G2D, CD11c, or F4/80 in spleen and LNs from *Pla2g2d*$^{+/+}$ (+/+) and *Pla2g2d*$^{-/-}$ (−/−) mice. (F) The AutoMACS-sorted splenic CD11c$^+$ cells were sorted for MHC class II by FACS (right), and then analyzed for expression of *Pla2g2d* relative to *Rn18s* (mean ± SEM from four mice, a representative of two experiments; left). (G) Immunohistochemistry of human LNs with anti–human PLA2G2D or control antibody. A boxed area is magnified. Arrows indicate PLA2G2D$^+$ cells. (H) Confocal immunofluorescence microscopy of PLA2G2D and CD11c in human LNs. (I and J) AutoMACS-sorted CD11c$^+$ cells from mouse splenocytes were further FACS-sorted for CD11b (I) or CD4 and CD8 (J; right), and then examined for expression of *Pla2g2d* relative to *Rn18s* (mean ± SEM from four mice, representative results from three experiments; left). (K) Expression of *Pla2g2d* relative to *Rn18s* in CD4$^+$, CD8$^+$, or CD4$^+$CD25$^+$ T cells and CD11c$^+$ cells (a representative of two experiments). FACS profiles are representative of two (F) or three (I and J) experiments. Images are representative of two (H) or three (C, E, and G) experiments.

Downloaded from jem.rupress.org on August 18, 2013

Published May 20, 2013

To accurately determine the cellular type(s) in which PLA2G2D is expressed, mouse splenocytes were sorted into $CD11c^+$ and $CD11c^-$ cells, and the $CD11c^-$ population was further sorted for CD3ε (a T cell marker), CD45R (a B cell marker), and CD11b (a macrophage marker; Fig. S1). Quantitative RT-PCR revealed that *Pla2g2d* was enriched in the $CD11c^+$ fraction (Fig. 1 D), suggesting that PLA2G2D is expressed in lymphoid tissue-resident $CD11c^+$ cells of the mononuclear phagocyte lineage, including DCs and a subset of macrophages. In comparison, *Pla2g5*, which was detected in mouse spleen at a lower level, was distributed in $CD11b^+CD11c^-$ macrophages, whereas *Pla2g1b*, *Pla2g2a* (absent in C57BL/6 mice because of a natural mutation), *Pla2g2e*, *Pla2g2f*, and *Pla2g10* were hardly detected in these cells (Fig. 1, B and D). When mouse spleen and LNs were subjected to confocal immunofluorescence microscopy, PLA2G2D was largely colocalized with CD11c and only partially with F4/80, a genuine macrophage marker (Fig. 1 E), indicating that it is expressed in $CD11c^+$ DCs and a subpopulation of $CD11c^+$ $F4/80^+$ macrophages. Further sorting of the AutoMACS-sorted $CD11c^+$ cells revealed the distribution of *Pla2g2d* in MHC class II^{lo} cells in preference to MHC class II^{hi} cells (Fig. 1 F), suggesting that PLA2G2D is mainly expressed in DCs of low activation state and is down-regulated in DCs undergoing activation (also see below). Staining of PLA2G2D was also found in human LNs, where it was distributed in cells within the paracortical area and was colocalized with CD11c (Fig. 1 G, H).

In mouse spleen, lymphoid-resident conventional DCs are subdivided into three major subsets, including $CD11b^+$ $CD4^+CD8\alpha^-$ DCs ($CD4^+$ DCs), $CD11b^-CD8\alpha^+$ DCs ($CD8\alpha^+$ DCs), and $CD11b^+CD4^-CD8\alpha^-$ DCs ($CD4^-CD8\alpha^-$ DCs; Vremec et al., 2000; Tamura et al., 2005). When the AutoMACS-sorted $CD11c^+$ cells were further FACS-sorted for CD11b, *Pla2g2d* mRNA was enriched in the $CD11b^+$ population (Fig. 1 I). FACS sorting of another pool of $CD11c^+$ cells for CD4 and CD8α showed more abundant expression of *Pla2g2d* in $CD4^+$ DCs than in $CD8\alpha^+$ or $CD4^-CD8^-$ DCs (Fig. 1 J). Thus, among the conventional DCs, PLA2G2D is preferentially expressed in the $CD11b^+CD4^+CD8\alpha^-$ DC subset. Because PLA2G2D is expressed in T reg cells (von Allmen et al., 2009), we compared the expression of *Pla2g2d* in $CD11c^+$ cells and $CD4^+CD25^+$ T reg cells in mouse spleen. Among T cells, *Pla2g2d* was enriched in $CD4^+CD25^+$ T reg cells relative to total $CD4^+$ and $CD8\alpha^+$ T cells, as previously reported (von Allmen et al., 2009). However, its expression was markedly higher in $CD11c^+$ cells than in T reg cells (Fig. 1 K).

Generation of *Pla2g2d*$^{-/-}$ mice

To investigate the roles of PLA2G2D in vivo, we generated *Pla2g2d*$^{-/-}$ mice by gene targeting. Construction of the *Pla2g2d* targeting vector is illustrated in Fig. 2 A. Appropriately targeted ES cell clones were used to obtain chimeric mice that transmitted the targeted locus through the germ line. Male mice carrying a targeted *Pla2g2d* gene were crossed with female *CAG-Cre* transgenic mice, which allowed deletion of exons 2 and 3 from the *Pla2g2d* gene in all tissues. Heterozygous mice carrying a mutated *Pla2g2d* allele (*Pla2g2d*$^{+/-}$) were backcrossed onto the C57BL/6 background ($n > 12$). Successful ablation of the *Pla2g2d* gene was confirmed by PCR genotyping from tail biopsy (Fig. 2 B) and by the absence of its mRNA (Fig. 2 C) and protein (Fig. 2 D) in the LNs and spleen of *Pla2g2d*$^{-/-}$ mice as demonstrated by quantitative RT-PCR and immunoblotting, respectively. Also, PLA2G2D staining was absent in the LNs of *Pla2g2d*$^{-/-}$ mice (Fig. 1 E), confirming the specificity of the anti-PLA2G2D antibody used here.

The ratio of the genotypes of heterozygous male and female offspring exhibited Mendelian proportions, and homozygous null mice were indistinguishable from WT littermates in terms of survival rates, appearance, fertility, and gross behavior, suggesting that the lack of PLA2G2D did not affect embryonic and postnatal development in normal states. The serum levels of biomedical markers and the proportions of blood cells were similar between the genotypes (Tables S1 and S2). DC, T cell, B cell, and macrophage populations in spleen, inguinal, and mesenteric LNs, Peyer's patch, and thymus were indistinguishable between *Pla2g2d*$^{-/-}$ and *Pla2g2d*$^{+/+}$ mice, except that the splenic proportion of $CD4^+$ T cells was slightly greater in *Pla2g2d*$^{-/-}$ mice (Fig. 2, E–G). Thus, PLA2G2D ablation did not profoundly affect hematopoiesis or lymphopoiesis under normal conditions. LN expression of other PLA_2s was similar between the genotypes (unpublished data), confirming that the lack of PLA2G2D was not compensated by other PLA_2s.

Impaired resolution of hapten-induced CHS in *Pla2g2d*$^{-/-}$ mice

To assess the immunoregulatory role of PLA2G2D in vivo, *Pla2g2d*$^{-/-}$ mice and WT littermates were subjected to hapten-induced CHS. In this well-known model for Th1 response, application of the hapten antigen dinitrofluorobenzene (DNFB) onto abdominal skin (sensitization), followed by the second application of the same antigen onto ear skin (elicitation) induced ear swelling. In normal skin, there are resident $CD11c^+$ populations including epidermal Langerhans cells and dermal DCs, which capture antigen and migrate into draining LNs (Heath and Carbone, 2009). Although *Pla2g2d* expression was low in nonlymphoid tissues (Fig. 1 A), confocal microscopy of the ear revealed that scattered PLA2G2D signal was colocalized in dermal and to a lesser extent in epidermal $CD11c^+$ cells in WT mice, while it was absent in *Pla2g2d*$^{-/-}$ skin (Fig. 3 A). Inflammation recruits monocytes that are differentiated into $CD11c^+$ inflammatory DCs or macrophages, which act as a peripheral stimulator of T cells (Heath and Carbone, 2009). Remarkably, cells expressing both PLA2G2D and CD11c were increased in the dermis and even epidermis after DNFB challenge for 24 h (Fig. 3 A), indicating that PLA2G2D is also expressed in many, if not all, inflammatory DCs or macrophages migrating into the inflamed skin.

Downloaded from jem.rupress.org on August 18, 2013

Published May 20, 2013

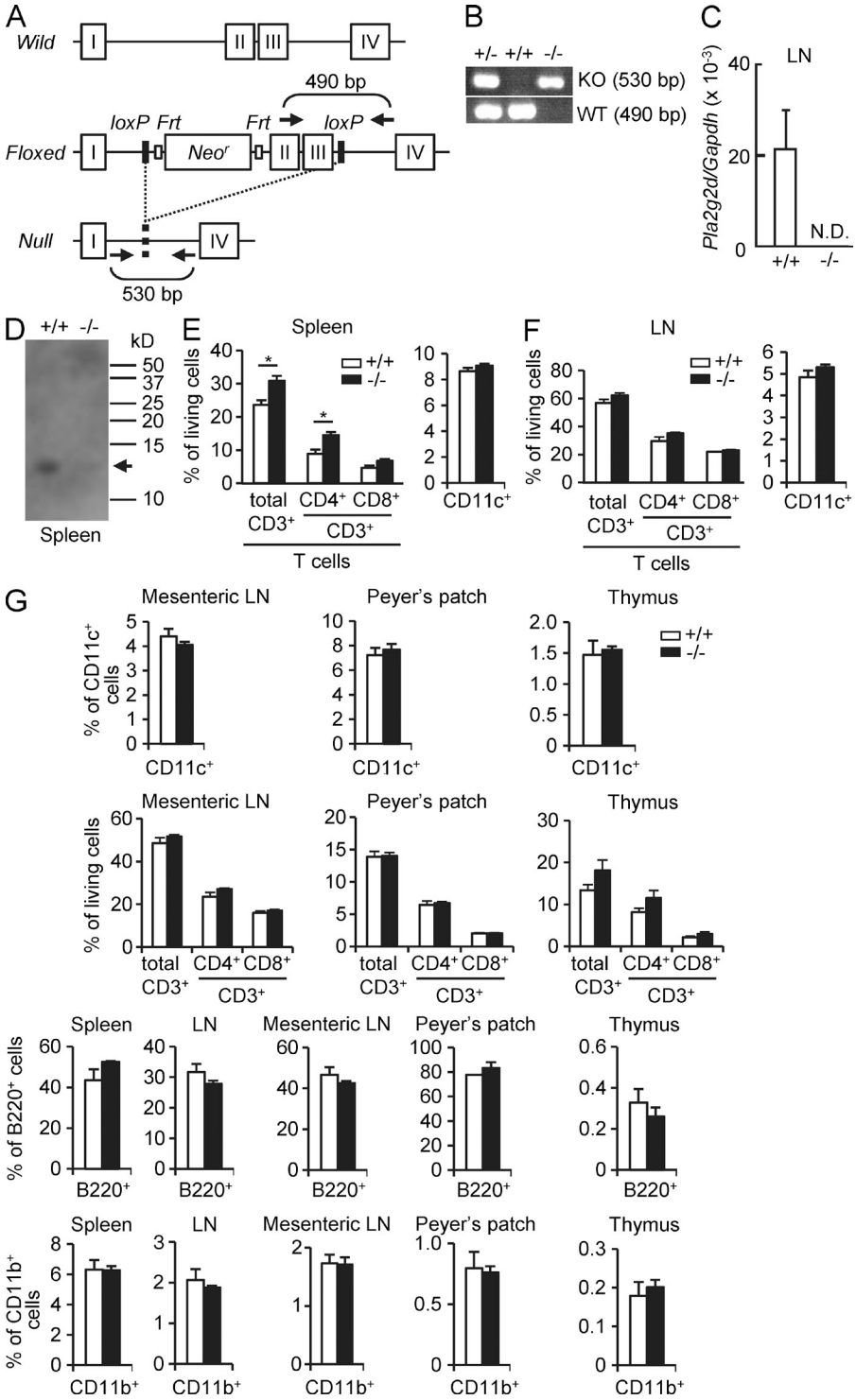

Figure 2. Gene targeting of *Pla2g2d*. (A) Strategy for gene targeting of the *Pla2g2d* gene. Positions of PCR primers for genotyping are indicated. (B) An example of PCR genotyping of *Pla2g2d*$^{+/+}$, *Pla2g2d*$^{+/-}$, and *Pla2g2d*$^{-/-}$ mice. (C) Quantitative RT-PCR of *Pla2g2d* expression in the inguinal LNs of *Pla2g2d*$^{+/+}$ and *Pla2g2d*$^{-/-}$ mice (mean ± SEM from four mice per group). (D) Western blotting of PLA2G2D protein in the spleen of *Pla2g2d*$^{+/+}$ and *Pla2g2d*$^{-/-}$ mice. Arrow indicates the position of 14-kD PLA2G2D protein. A representative blot of three experiments is shown. (E and F) Proportions of T cells and DCs in spleen (E) and inguinal LNs (F) were determined by FACS (mean ± SEM from three mice per group; *, $P < 0.05$). (G) Immune cells from the indicated tissues from *Pla2g2d*$^{+/+}$ and *Pla2g2d*$^{-/-}$ mice were subjected to FACS analysis to examine the populations of CD11c$^+$ DCs, CD3ε^+ T cells (both CD4$^+$ and CD8$^+$ populations), CD45R$^+$ (B220$^+$) B cells, and CD11b$^+$ monocytes/macrophages (mean ± SEM from three mice per group). Representative results of two experiments are shown in (B, C, and E–G). In C–G, 7-wk-old male mice were used.

We then compared the process of CHS between *Pla2g2d*$^{+/+}$ and *Pla2g2d*$^{-/-}$ mice. In WT mice, ear swelling peaked by day 3 and declined to nearly the basal level by day 6 after DNFB challenge (Fig. 3 B). At lower doses of DNFB, milder edema peaked on days 2–3, and then shifted to the declining phase (Fig. 3 C), confirming that the onset and resolution were not affected by the intensity of the stimulus. The initial process of ear swelling by day 3 occurred normally in *Pla2g2d*$^{-/-}$ mice, with no significant difference from *Pla2g2d*$^{+/+}$ mice. After reaching the peak, ear edema in *Pla2g2d*$^{-/-}$ mice continued to maintain the maximally exaggerated state by day 5, and then decayed at a slower rate by day 10, at which time the ear was still thicker than in WT mice (Fig. 3 B), implying a delayed resolution in the null mice. In accordance, histological

Downloaded from jem.rupress.org on August 18, 2013

Published May 20, 2013

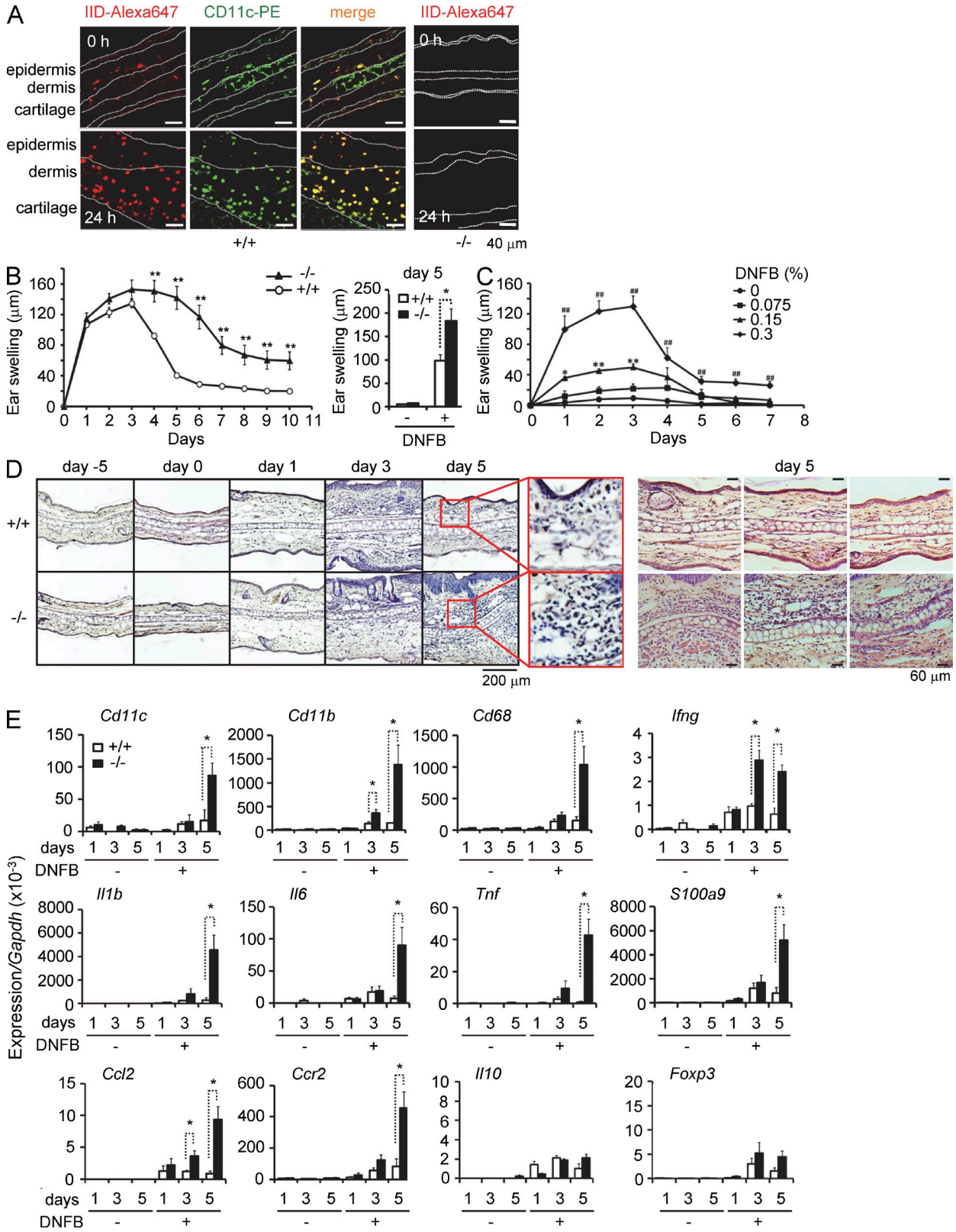

Figure 3. Impaired resolution of skin inflammation in *Pla2g2d*$^{-/-}$ mice in a DNFB-induced CHS model. (A) Confocal immunofluorescence microscopy of PLA2G2D (IID-Alexa647; *red*) and CD11c (CD11c-PE; *green*) in ear skin from *Pla2g2d*$^{+/+}$ (+/+) and *Pla2g2d*$^{-/-}$ (−/−) mice before and 24 h after elicitation of DNFB-induced CHS. Green signal in the cartilage is nonspecific. Images are representative of two experiments. (B) Monitoring of ear thickness over the elicitation period of CHS in *Pla2g2d*$^{+/+}$ and *Pla2g2d*$^{-/-}$ mice (left). Result is a representative of three experiments (mean ± SEM from 7

Downloaded from jem.rupress.org on August 18, 2013

Published May 20, 2013

examination of the ears showed more severe ear swelling, epidermal hyperplasia, and inflammatory cell infiltration in *Pla2g2d*$^{-/-}$ mice than in *Pla2g2d*$^{+/+}$ mice on day 5 (Fig. 3 D).

Quantitative RT-PCR of ear skin revealed that the expression levels of inflammatory markers, including *Cd11c*, *Cd11b*, and *Cd68* (surface markers of inflammatory DCs or macrophages), *Ifng* (IFN-γ; a Th1 cytokine), *Il1b*, *Il6*, and *Tnf* (IL-1β, IL-6, and TNF; proinflammatory cytokines), *Ccl2*, and *Ccr2* (a monocyte-attracting chemokine and its receptor), and *S100a9* (a marker of epidermal hyperplasia) peaked by day 3, and then declined by day 5 in *Pla2g2d*$^{+/+}$ mice, whereas they were dramatically increased on day 5 in *Pla2g2d*$^{-/-}$ mice (Fig. 3 E). A robust increase of *Ifng* in *Pla2g2d*$^{-/-}$ mice over *Pla2g2d*$^{+/+}$ mice became obvious on day 3 before that of other proinflammatory markers, implying that the exacerbated inflammation in the null mice stemmed from the augmented Th1 response (Lu et al., 1998). In contrast, expression levels of *Il10* (IL-10), an antiinflammatory cytokine (Fickenscher et al., 2002), and of *Foxp3*, a marker of T reg cells (Shevach, 2009), in *Pla2g2d*$^{-/-}$ skin did not differ significantly from those in *Pla2g2d*$^{+/+}$ skin throughout the experimental periods (Fig. 3 E), suggesting that T reg cell migration or proliferation in the inflamed skin was unaffected by PLA2G2D deficiency. Thus, during the resolution process of CHS, a cytokine milieu in the affected skin is skewed toward a proinflammatory profile rather than an antiinflammatory profile in *Pla2g2d*$^{-/-}$ mice.

We also examined the inflammatory status in the draining LNs during the elicitation phase of CHS. After DNFB challenge to the ears, *Pla2g2d* expression in the LNs of WT mice was increased on days 1 to 5 (Fig. 4 A), reaching a much higher level than in the skin (Fig. 4 B). The modest increase of *Pla2g2d* was accompanied by a concomitant increase of *Cd11c* and a robust increase of *Ifng* on days 1–3 (Fig. 4 A). Subsequently, the expressions of *Cd11c* and *Ifng* were declined to their basal levels by day 5 in *Pla2g2d*$^{+/+}$ mice, underscoring the resolution of LN inflammation. In *Pla2g2d*$^{-/-}$ LNs, however, the expression levels of *Cd11c* and *Ifng* still remained at their highest levels on day 5 (Fig. 4 A). On day 5, CD11c^{+}MHC class II^{+} activated DCs (Fig. 4 C) and CD3ε^{+} CD44^{+}CD62L^{-} effector T cells (Fig. 4 D) were greater in *Pla2g2d*$^{-/-}$ LNs than in *Pla2g2d*$^{+/+}$ LNs. Thus, as in the affected skin, inflammation failed to resolve in the draining LNs of DNFB-challenged *Pla2g2d*$^{-/-}$ mice relative to *Pla2g2d*$^{+/+}$ mice.

LN cells were harvested from DNFB-sensitized *Pla2g2d*$^{-/-}$ and *Pla2g2d*$^{+/+}$ mice and cultured for 24 h ex vivo in the presence of dinitrobenzene sulfonic acid (DNBS; a water-soluble form of DNFB). Expression levels of the Th1 cytokines *Ifng* and *Il12a* were markedly higher in *Pla2g2d*$^{-/-}$ LN cells than in WT cells, whereas those of the antiinflammatory cytokines *Tgfb* and *Il10*, as well as the T reg cell marker *Foxp3*, were unaffected by the absence of PLA2G2D (Fig. 4 E). In agreement, the elevated secretion of IFN-γ, but not IL-10, in the culture of *Pla2g2d*$^{-/-}$ LN cells relative to *Pla2g2d*$^{+/+}$ LN cells over time was confirmed by ELISA (Fig. 4 F), and the unaltered CD4^{+}FoxP3^{+} T reg cell population in *Pla2g2d*$^{-/-}$ LNs was confirmed by flow cytometry (Fig. 4 G). These results indicate again that the proinflammatory signal exceeds the antiinflammatory signal in *Pla2g2d*$^{-/-}$ LNs compared with *Pla2g2d*$^{+/+}$ LNs. However, our results do not support the proposal that PLA2G2D facilitates the expansion and immunosuppressive function of T reg cells (von Allmen et al., 2009), at least in the CHS model used here.

To verify whether PLA2G2D deficiency did not affect the initial process of CHS, we examined the migration of skin-resident DCs into the draining LNs during the sensitization phase. After capture of a foreign antigen, skin-resident DCs are activated and migrate into the regional LNs, where they present the antigen to T cells (Heath and Carbone, 2009). The fluorescent hapten antigen FITC was topically applied onto the skin of *Pla2g2d*$^{+/+}$ and *Pla2g2d*$^{-/-}$ mice, and then the migration of FITC-captured skin DCs into the draining LNs was monitored by flow cytometry. The proportion of FITC^{+}CD11c^{+} or FITC^{+}MHC class II^{+} DCs was similar between *Pla2g2d*$^{+/+}$ and *Pla2g2d*$^{-/-}$ LNs (Fig. 4, H and I), implying that the lack of PLA2G2D does not affect antigen uptake, recruitment, and activation of skin DCs migrating into the LNs. Notably, many of the FITC^{+}CD11c^{+} cells in the LNs did not display PLA2G2D signal (Fig. 4 J), suggesting that PLA2G2D expression was decreased after activation and LN recruitment of skin DCs. Thus, the apparent effect of PLA2G2D deficiency is restricted to the late period of CHS.

Pla2g2d$^{-/-}$ DCs are hyperactivated

To assess whether the increased immune responses in *Pla2g2d*$^{-/-}$ mice is attributable to some abnormalities in DCs, we analyzed GM-CSF–driven BM-derived DCs (CD11b^{+}CD11c^{+} BMDCs; McGeachy, 2011). Although the expression of *Pla2g2d* was minimal in BM cells, it was robustly induced in GM-CSF-driven BMDCs (Fig. 5 A). Compared with BMDCs, *Pla2g2d* expression in M-CSF–driven BM-derived macrophages (CD11b^{+} CD11c^{-} BMDMs) was low (Fig. 5 B), agreeing with the preferential expression of PLA2G2D in CD11c^{+} DCs in vivo. When BMDCs or even BMDMs were treated for 24 h with LPS, *Pla2g2d* expression was reduced markedly (Fig. 5, A and B),

Pla2g2d$^{+/+}$ and 8 *Pla2g2d*$^{-/-}$ mice per group; **, P < 0.01). (right) Pooled data on day 5 from three experiments (mean ± SEM from 12 mice per group without DNFB or 21 (+/+) and 23 (−/−) mice with DNFB; *, P < 0.05). (C) Monitoring of ear thickness after treatment of WT mice with various doses of DNFB (mean ± SEM from 5 mice per group; *, P < 0.05 and **, P < 0.01, 0 versus 0.15% DNFB; #, P < 0.01, 0% versus 0.3% DNFB; representative of three experiments). (D) Hematoxylin/eosin staining of ear skin sections obtained at the indicated times from *Pla2g2d*$^{+/+}$ and *Pla2g2d*$^{-/-}$ mice. Images are representative of four experiments. The ears on day 5 are magnified (red boxes). Other examples of ear histology on day 5 are also shown (right). (E) Quantitative RT-PCR of various pro- and antiinflammatory marker genes relative to *Gapdh* in the ear skins of *Pla2g2d*$^{+/+}$ and *Pla2g2d*$^{-/-}$ mice at the indicated time points. Data are representative of three experiments (mean ± SEM from 3 mice without DNFB and four mice with DNFB per group; *P < 0.05).

Downloaded from jem.rupress.org on August 18, 2013

Published May 20, 2013

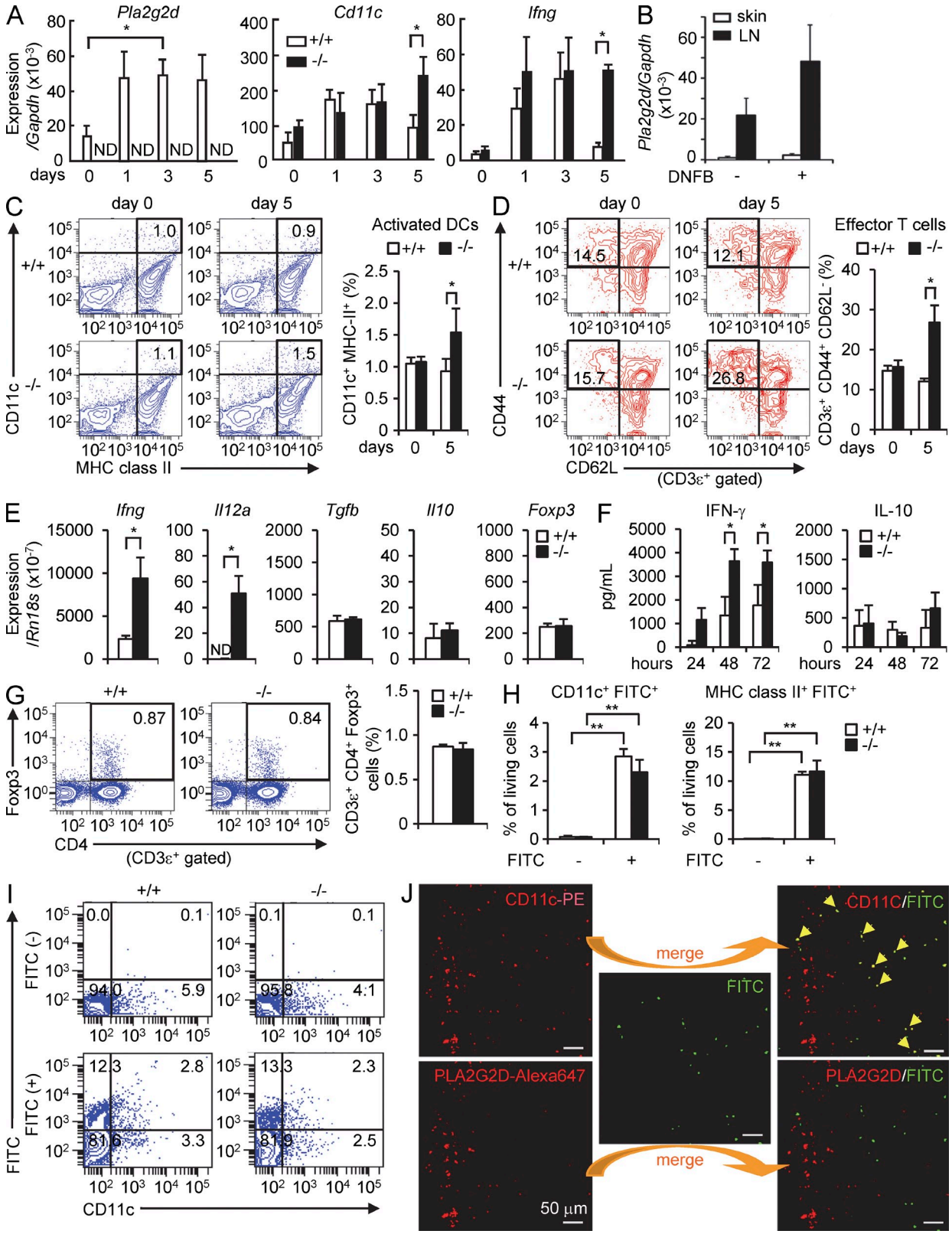

Figure 4. Impaired resolution of LN inflammation in *Pla2g2d*$^{-/-}$ mice in a DNFB-induced CHS model. (A) Quantitative RT-PCR of *Pla2g2d*, *Cd11c*, and *Ifng* relative to *Gapdh* in the LNs of *Pla2g2d*$^{+/+}$ (+/+) and *Pla2g2d*$^{-/-}$ (−/−) mice during the elicitation phase of CHS (mean ± SEM from four mice per group). (B) Quantitative RT-PCR of *Pla2g2d* relative to *Gapdh* in the ear skin and LNs of *Pla2g2d*$^{+/+}$ and *Pla2g2d*$^{-/-}$ mice on day 5 with or without DNFB challenge (mean ± SEM from four mice per group). (C and D) FACS for activated DCs (CD11c^{+}MHC class II^{+}; C) and effector T cells

Downloaded from jem.rupress.org on August 18, 2013

Published May 20, 2013

a finding reminiscent of its down-regulation by LPS in mouse tissues (Suzuki et al., 2000; von Allmen et al., 2009) and human macrophages (Lindbom et al., 2005). Thus, corroborating with the data shown in Figs. 1 F and 4 J, PLA2G2D expression inversely correlates with DC activation.

Even without stimulation, *Pla2g2d*$^{-/-}$ BMDCs had greater surface expression of MHC class II, CD80, and CD86 than *Pla2g2d*$^{+/+}$ BMDCs (Fig. 5 C). Further incubation with a suboptimal concentration of LPS increased more CD11b^{+} MHC class II^{+} (Fig. 5 D) and CD80^{+}CD86^{+} (Fig. 5 E) BMDCs from *Pla2g2d*$^{-/-}$ mice than from *Pla2g2d*$^{+/+}$ mice. There were substantial increases in IL-6 and TNF secretion from *Pla2g2d*$^{-/-}$ BMDCs over *Pla2g2d*$^{+/+}$ BMDCs in response to suboptimal LPS (Fig. 5 F). Moreover, when C57BL/6 mice were intravenously transferred with *Pla2g2d*$^{+/+}$ or *Pla2g2d*$^{-/-}$ BMDCs that had been sensitized with DNBS, and then subjected to DNFB challenge, mice transferred with *Pla2g2d*$^{-/-}$ BMDCs exhibited greater edema than those transferred with *Pla2g2d*$^{+/+}$ BMDCs (Fig. 5 G). Thus, PLA2G2D deficiency allows BMDCs to be hyperactivated, leading to more severe inflammation.

Altered lipid profiles in the LNs of *Pla2g2d*$^{-/-}$ mice

Because PLA2G2D is a lipolytic enzyme, we speculated that the impaired resolution of CHS in *Pla2g2d*$^{-/-}$ mice might result from some perturbed lipid metabolisms. We therefore performed electrospray ionization mass spectrometry (ESI-MS) to comprehensively monitor the levels of free PUFAs and their oxygenated metabolites in the draining LNs and skin of *Pla2g2d*$^{-/-}$ mice in comparison with *Pla2g2d*$^{+/+}$ mice on day 5 after DNFB challenge, a time point when *Pla2g2d*$^{-/-}$ mice exhibited an impaired resolution of inflammation.

Bioactive metabolomes for AA-, EPA-, and DHA-derived products revealed that DNFB challenge led to substantial increases in free AA, EPA, and DHA, with concomitant increases in many if not all of their bioactive metabolites, in the LNs of *Pla2g2d*$^{+/+}$ mice. Remarkably, the levels of AA, EPA, and DHA were significantly lower in *Pla2g2d*$^{-/-}$ LNs than in *Pla2g2d*$^{+/+}$ LNs in the presence or even in the absence of DNFB challenge (Fig. 6 A), suggesting that PLA2G2D plays a role in the constitutive and inducible supply of a large portion of these PUFAs in the LNs. However, the levels of many AA metabolites, including the cyclooxygenase products PGE_2, $PGF_{2\alpha}$, 6-keto-$PGF_{1\alpha}$ (an end-product of PGI_2), and thromboxane (TX) B_2 (an end-product of TXA_2), as well as the 5-lipoxygenase product 5-hydroxyeicosatetraenoic acid (HETE), some of which promote Th1-dominated inflammation (Byrum et al., 1999; Kabashima et al., 2003; Nagamachi et al., 2007; Yao et al., 2009; Nakajima et al., 2010), did not differ significantly between the genotypes in DNFB-treated and -untreated settings (Fig. 6 B). In contrast, the DNFB-induced increases in the AA-derived antiinflammatory prostanoid 15d-PGJ_2 and its precursor PGD_2 occurred only partially in *Pla2g2d*$^{-/-}$ mice relative to *Pla2g2d*$^{+/+}$ mice (Fig. 6 C). These results suggest that the PLA2G2D-sensitive AA pool is preferentially coupled with the antiinflammatory PGD_2/15d-PGJ_2 axis, whereas another AA pool remaining in *Pla2g2d*$^{-/-}$ mice, which may be supplied by $cPLA_2\alpha$ (Bonventre et al., 1997; Uozumi et al., 1997), is sufficient for full mobilization of the proinflammatory AA metabolites.

In addition, the EPA and DHA bioactive metabolomes revealed that the levels of ω-3 EPA- and DHA-derived metabolites, which included the potent pro-resolving lipid mediator resolvin D1 (RvD1), were considerably lower in *Pla2g2d*$^{-/-}$ LNs than in *Pla2g2d*$^{+/+}$ LNs regardless of DNFB challenge (Fig. 6 D). Thus, along with the reduction in the inducible production of ω-6 AA-derived 15d-PGJ_2 (Fig. 6 C), the absence of PLA2G2D causes a marked reduction in the steady-state levels of ω-3 PUFAs and their enzymatically oxygenated products. The lipidomic profile on day 1, an early peak point of CHS, was similar to that on day 5 (Fig. 6 E). Hence, the constitutive supply of pro-resolving lipid mediators by PLA2G2D may be important for the early entry into resolution, rather than for limiting the maximal inflammatory response. To obtain a possible explanation for these changes in lipid profiles in *Pla2g2d*$^{-/-}$ LNs, we examined the expression of downstream enzymes responsible for the conversion of PUFAs to bioactive metabolites. Notably, the expression levels of prostanoid-biosynthetic enzymes tended to be higher in *Pla2g2d*$^{-/-}$ LNs than in *Pla2g2d*$^{+/+}$ LNs, whereas that of 12/15-lipoxygenase, an enzyme crucial for the conversion of ω-3 PUFAs to anti-inflammatory lipid mediators, was similar in both genotypes (Fig. 6 F). Thus, in *Pla2g2d*$^{-/-}$ LNs, the diminished supply of AA might be counter-balanced by the elevated expression of downstream enzymes for proinflammatory lipid mediators, while the reduction of ω-3 PUFAs might be linked to the reduction of pro-resolving lipid mediators because of the lack of compensatory up-regulation of 12/15-lipoxygenase.

Lipidomics analysis of the affected skin on day 5 of CHS revealed that none of the free PUFAs and their metabolites were significantly altered in *Pla2g2d*$^{-/-}$ mice relative to *Pla2g2d*$^{+/+}$

(CD3ε^{+}CD44^{+}CD62L^{-}; D) in the LNs of *Pla2g2d*$^{+/+}$ and *Pla2g2d*$^{-/-}$ mice. Representative FACS profiles and average scores (mean ± SEM from three mice per group) are shown. (E and F) LN cells harvested from DNFB-sensitized *Pla2g2d*$^{+/+}$ and *Pla2g2d*$^{-/-}$ mice on day 0 were cultured with 100 µg/ml DNBS ex vivo to assess the expression of pro- and antiinflammatory markers at 24 h by quantitative RT-PCR (E) or the secretion of cytokines over 72 h by ELISA (F; mean ± SEM from four mice per group). (G) FACS for CD4 and FoxP3 on CD3ε^{+}-gated T cells from *Pla2g2d*$^{+/+}$ and *Pla2g2d*$^{-/-}$ LNs on day 5. Representative FACS profiles and average scores (mean ± SEM from four mice per group) are shown. (H and I) FACS for FITC in combination with CD11c or MHC class II in skin-draining LNs 24 h after treatment of the abdominal skins of *Pla2g2d*$^{+/+}$ and *Pla2g2d*$^{-/-}$ mice with 200 µl of 1% FITC in acetone/dibutyl phthalate (1:1). Average scores of FITC^{+}CD11c^{+} or FITC^{+}MHC class II^{+} cells (mean ± SEM from four mice per group; H) and representative FACS profiles (I) are shown. (J) A representative images of confocal microscopy of PLA2G2D, CD11c, and FITC in the LNs of WT mice used in (H and I). Arrowheads indicate the cells in which CD11c and FITC signals were colocalized. Results are representative of two (C–J) or three (A and B) experiments. *, $P < 0.05$; **, $P < 0.01$.

Downloaded from jem.rupress.org on August 18, 2013

Published May 20, 2013

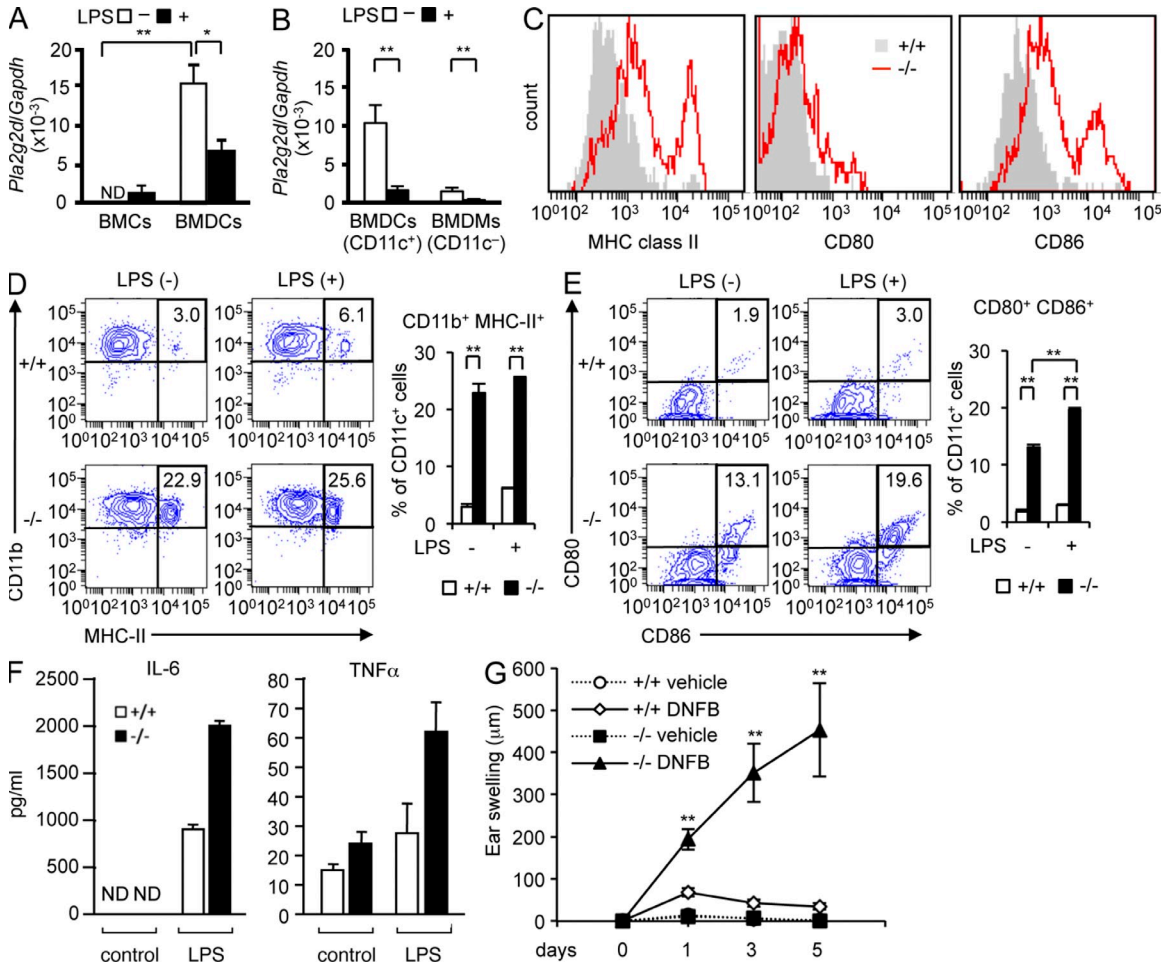

Figure 5. Absence of PLA2G2D hyperactivates BMDCs. (A and B) Quantitative RT-PCR of *Pla2g2d* relative to *Gapdh* in BM cells (BMCs), BMDCs, and BMDMs from WT mice, with or without stimulation with 1 μg/ml LPS (mean ± SEM from 3 (A) and 5 (B) mice per group). (C) FACS profiles of CD11c-gated BMDCs from *Pla2g2d*$^{+/+}$ (+/+) and *Pla2g2d*$^{-/-}$ (−/−) mice for surface expression of MHC class II, CD80, and CD86. (D and E) Representative FACS profiles and average scores (mean ± SEM from three mice per group) for surface expression of CD11b and MHC class II (D) or CD80 and CD86 (E) in *Pla2g2d*$^{+/+}$ and *Pla2g2d*$^{-/-}$ BMDCs with or without stimulation with 10 ng/ml LPS for 24 h. (F) Secretion of cytokines from *Pla2g2d*$^{+/+}$ and *Pla2g2d*$^{-/-}$ BMDCs treated for 24 h with or without 10 ng/ml LPS (mean ± SEM from three mice per group). (G) BMDCs from *Pla2g2d*$^{+/+}$ and *Pla2g2d*$^{-/-}$ mice were sensitized with DNBS and then intravenously transferred into C57BL/6 mice. After 5 d, DNFB was painted on the ear skin to monitor ear thickness over time (mean ± SEM from four mice per group). Data are representative of two (B and F) or three (A, C–E, and G) experiments. ND, not detected. *, $P < 0.05$; **, $P < 0.01$.

mice (Fig. 6 G). Thus, despite the increased skin inflammation, overall lipid mediator profiles in the skin were unaffected by PLA2G2D deficiency. Altogether, it is likely that PLA2G2D acts mainly in lymphoid tissues, where it supplies a particular pool of PUFAs that is selectively coupled with antiinflammatory/pro-resolving lipid mediator programs and thereby contributes to the resolution of CHS primarily in the LNs and secondarily in the skin.

PLA2G2D releases PUFAs from phosphatidylethanolamine in LN membranes

Having established that the deficiency of PLA2G2D reduces the LN levels of PUFAs such as AA and DHA, we next sought to gain insights into phospholipid subclasses from which PLA2G2D could release these PUFAs. To this end, we extracted total lipids from LNs and incubated them with or without recombinant mouse PLA2G2D protein. Then, the lipids were subjected to ESI-MS to analyze the reduction of phospholipid species and the increase of lysophospholipids and free fatty acids.

We found that PLA2G2D selectively decreased several diacyl and alkenyl forms of phosphatidylethanolamine (PE) molecular species containing unsaturated fatty acids, particularly those containing AA and DHA, whereas phosphatidylcholine (PC), phosphatidylinositol (PI), phosphatidylserine (PS), and phosphatidylglycerol (PG) species were barely affected by the enzyme (Fig. 7 A). The decreases of particular PE species by PLA2G2D were accompanied by concomitant increases in lysophosphatidylethanolamine (LysoPE) species with saturated or monounsaturated fatty acid (which are likely to be *sn*-1 bound), supporting the PLA_2 reaction (Fig. 7 B). In agreement with the unaltered PC and PS levels

Downloaded from jem.rupress.org on August 18, 2013

Published May 20, 2013

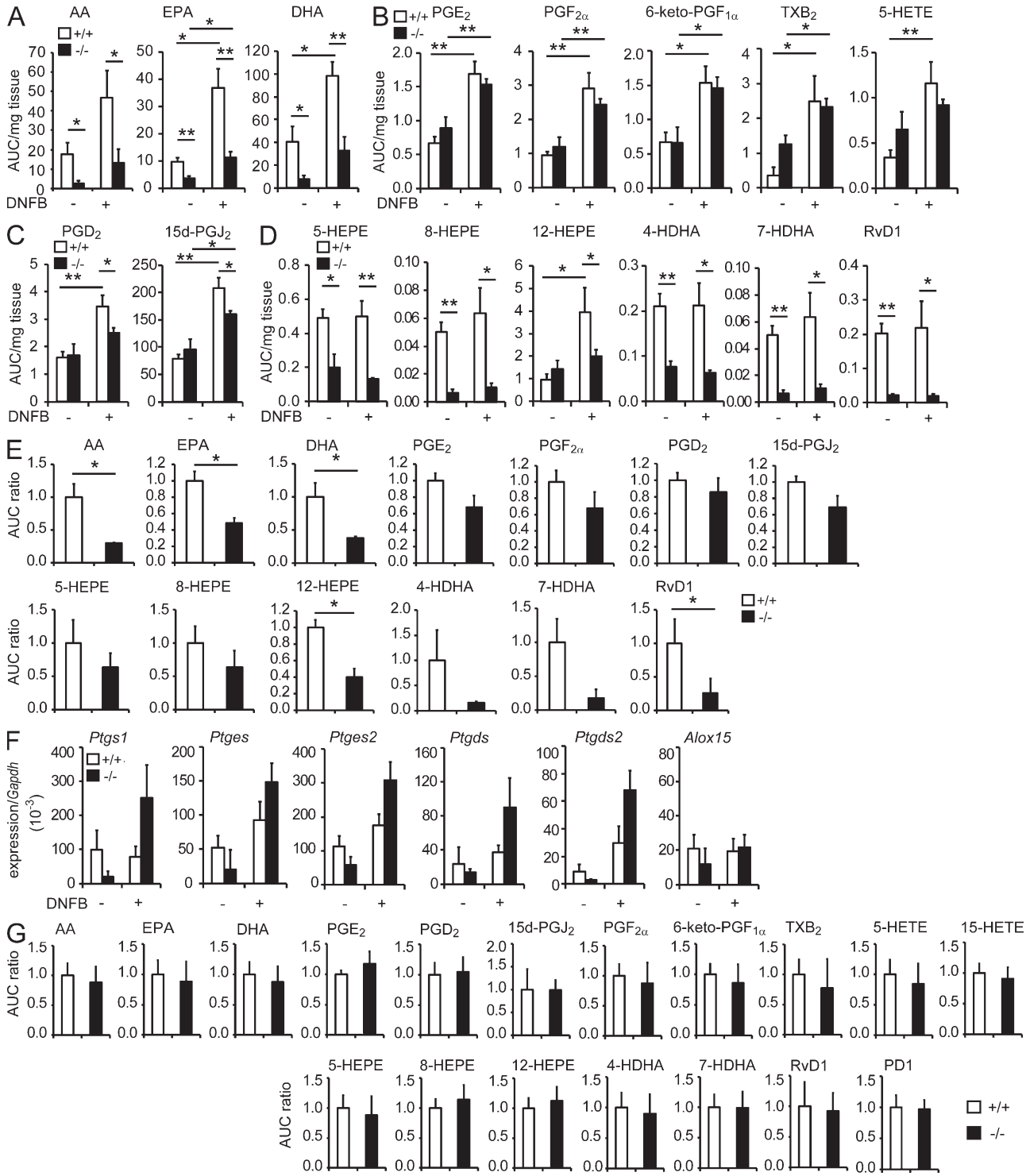

Figure 6. LC-ESI/MS profiling of PUFAs and their bioactive mediators. (A-D) LC-ESI/MS of free PUFAs (A), proinflammatory AA metabolites (B), antiinflammatory AA metabolites (C), and EPA or DHA metabolites (D) in the LNs of *Pla2g2d*$^{+/+}$ (+/+) and *Pla2g2d*$^{-/-}$ (−/−) mice on day 5 of CHS, with or without DNFB treatment (mean ± SEM from five mice per group). Values are AUC (area under the curve) per mg tissue, as evaluated by comparison with an internal standard (1 AUC = ~50 pg). (E) LC-ESI/MS of free PUFAs and their metabolites in the LNs of *Pla2g2d*$^{+/+}$ and *Pla2g2d*$^{-/-}$ mice on day 1 after DNFB challenge (mean ± SEM from three mice per group). (F) Quantitative RT-PCR of lipid mediator-biosynthetic enzymes relative to *Gapdh* in the LNs on day 5 after DNFB challenge (mean ± SEM from three mice per group). (G) LC-ESI/MS of free PUFAs and their metabolites in the ear skin of DNFB-challenged *Pla2g2d*$^{+/+}$ and *Pla2g2d*$^{-/-}$ mice on day 5 (mean ± SEM from 10 mice per group). In E and G, values are expressed as AUC ratio, with the level of each product in *Pla2g2d*$^{+/+}$ mice being regarded as 1. HEPE, hydroxyeicosapentaenoic acid; HDHA, hydroxydocosahexaenoic acid; PD1, protectin D1. Representative results of two (E and F) or three (A–D) experiments and pooled results of two experiments (G) are shown. *, $P < 0.05$; **, $P < 0.01$.

Downloaded from jem.rupress.org on August 18, 2013

Published May 20, 2013

(Fig. 7 A), there were no increases in lysophosphatidylcholine (LysoPC) and lysophosphatidylserine (LysoPS) species (Fig. 7 B). Among the PUFAs, DHA and AA were increased in marked preference to linoleic acid (LA; C18:2) after the treatment with PLA2G2D (Fig. 7 C), an observation that agreed with the selective reduction of PE species bearing DHA or AA (Fig. 7 A). Moreover, this PUFA preference in vitro was recapitulated by marked abundance of free DHA and AA relative to LA in the LNs in vivo (Fig. 7 D). These results collectively suggest that PLA2G2D selectively hydrolyzes PUFA-containing PE in LN membranes to provide DHA and AA.

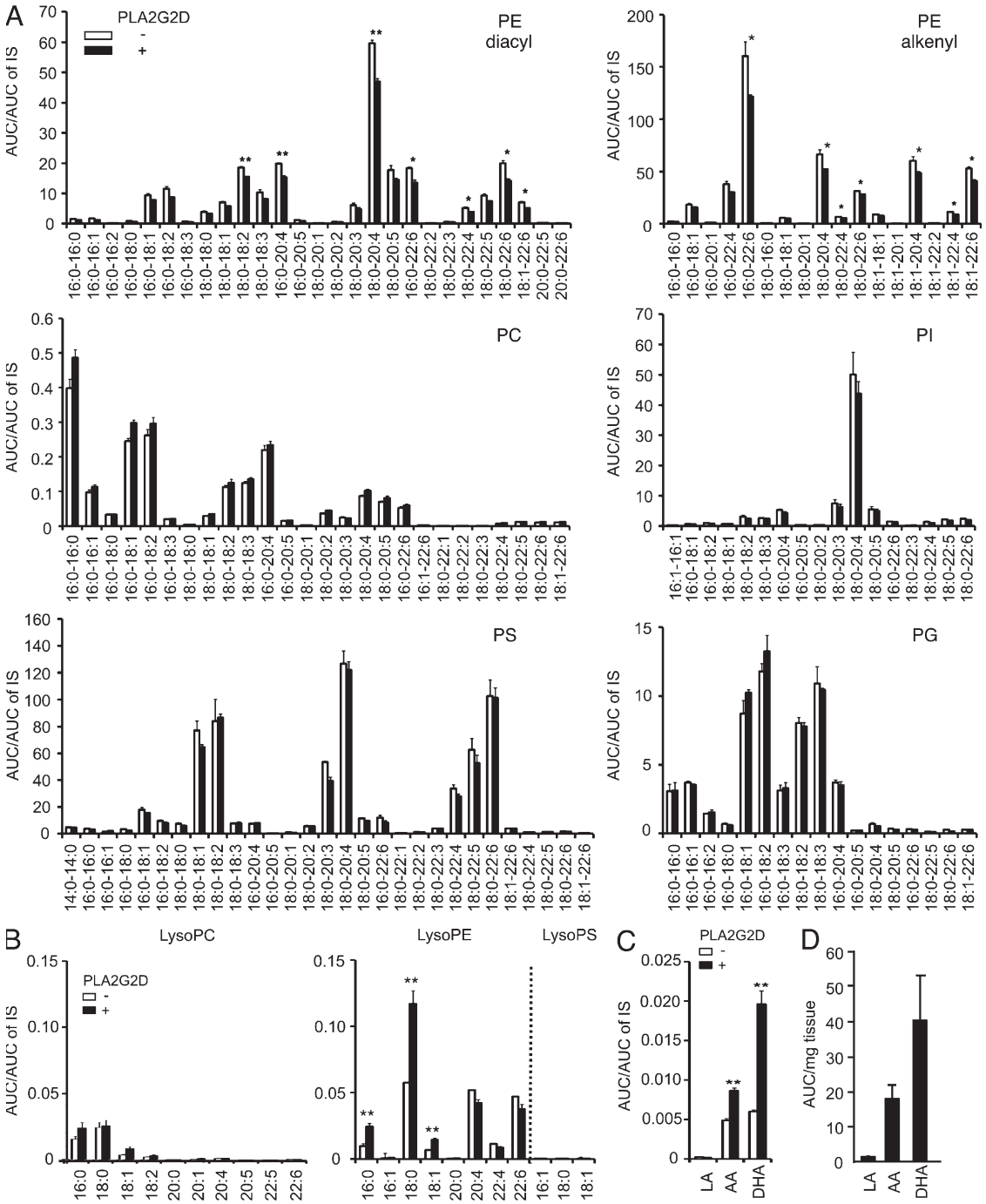

Figure 7. Hydrolysis of LN-derived phospholipids by recombinant PLA2G2D. (A–C) ESI-MS of phospholipids (A), lysophospholipids (B), and fatty acids (C) in total lipids extracted from the LNs and incubated with (+) or without (−) 200 nM recombinant mouse PLA2G2D (mean ± SEM, $n = 3$ per group). (D) ESI-MS of LA, AA, and DHA in the LNs of WT mice (mean ± SEM from five mice). Results in A–D are representative of three independent experiments. *, $P < 0.05$; **, $P < 0.01$.

Downloaded from jem.rupress.org on August 18, 2013

Published May 20, 2013

The lipid products altered in *Pla2g2d*$^{-/-}$ LNs dampen the DC-mediated immune responses

Finally, to assess whether the lipid products altered in *Pla2g2d*$^{-/-}$ LNs could indeed modulate the immune response, LN cells from DNFB-sensitized mice were stimulated with DNBS in the presence of the lipids. EPA, DHA, 15d-PGJ$_2$ and RvD1 dampened IFN-γ secretion, whereas LA and AA were ineffective (Fig. 8 A), confirming the immune regulation by the ω-3 PUFA products and the ω-6 cyclopentenone prostanoid. These antiinflammatory lipids also efficiently blocked IFN-γ production by *Pla2g2d*$^{-/-}$ LN cells (unpublished data). The levels of these lipids in WT LNs were estimated to be within a range of nanomolar to micromolar orders (Fig. 6 A), which were sufficient to block IFN-γ production by LN cells (Fig. 8 A). Furthermore, DHA, 15d-PGJ$_2$, and RvD1 reduced IL-12 secretion (Fig. 8 B) and surface expression of MHC class II (Fig. 8 C, D) in LPS-stimulated BMDCs. Together with previous studies reporting the antiinflammatory effects of ω-3 PUFAs on CHS models (Danno et al., 1993; Tomobe et al., 2000) and on DCs or macrophages (Groeger et al., 2010; Draper et al., 2011), our present results indicate that the lipid mediator balance is shifted toward a proinflammatory status in favor of an antiinflammatory status in *Pla2g2d*$^{-/-}$ LNs during the resolution phase of CHS.

DISCUSSION

Although the last decade has seen progress in deciphering the pathways that activates innate and acquired immunity, the mechanisms that limit these responses to secure homeostasis have not yet been fully defined. Antiinflammatory or pro-resolving lipid mediators can explain some of the beneficial actions of ω-3 PUFA-rich fish oils in various diseases (Yokoyama et al., 2007). Although the understanding of PUFA-oxygenated products with pro-resolving activities has recently been expanding (Serhan, 2007; Serhan et al., 2008), an interest in exploring the role of PLA$_2$s that can supply PUFA precursors upstream of their biosynthetic conversion to pro-resolving lipid mediators has emerged. Here, we have shown that PLA2G2D is an immunosuppressive sPLA$_2$ that is abundantly expressed in CD11c$^+$ cells in lymphoid organs and that its absence delays the resolution of CHS. Importantly, pro-resolving lipid mediators and their precursors were reduced in *Pla2g2d*$^{-/-}$ LNs, implying that PLA2G2D resolves inflammation by driving antiinflammatory lipid mediators in this tissue. Because of its pro-resolving role in CHS, along with a recent study showing an immunosuppressive effect of PLA2G2D-Fc fusion protein (von Allmen et al., 2009), we propose that PLA2G2D represents a "resolving sPLA$_2$" that mobilizes antiinflammatory or pro-resolving lipid mediators in lymphoid tissues.

PLA2G2D is mainly located in a cell population expressing CD11c, a molecular signature of DCs. DCs are antigen-presenting cells specialized to capture and process antigens for presentation on MHC products and then to control differentiation of T cells (Villadangos and Schnorrer, 2007), and they are highly diverged in terms of their locations, surface marker expressions, and functions (Heath and Carbone, 2009). Lymphoid-resident DCs present antigen that drains to LNs and stimulate the initial steps of T cell activation; migratory DCs transport antigen from peripheral tissues to regional LNs and stimulate the next steps of T cell activation; as immune stimulation continues, blood monocytes recruited to peripheral sites develop into inflammatory DCs, which migrate into LNs to provide a continuing stimulus for T cell activation; and TipDCs, another unique DC subset, mediate T cell–independent innate immune defense (Itano et al., 2003; Serbina et al., 2003; Allenspach et al., 2008;

Downloaded from jem.rupress.org on August 18, 2013

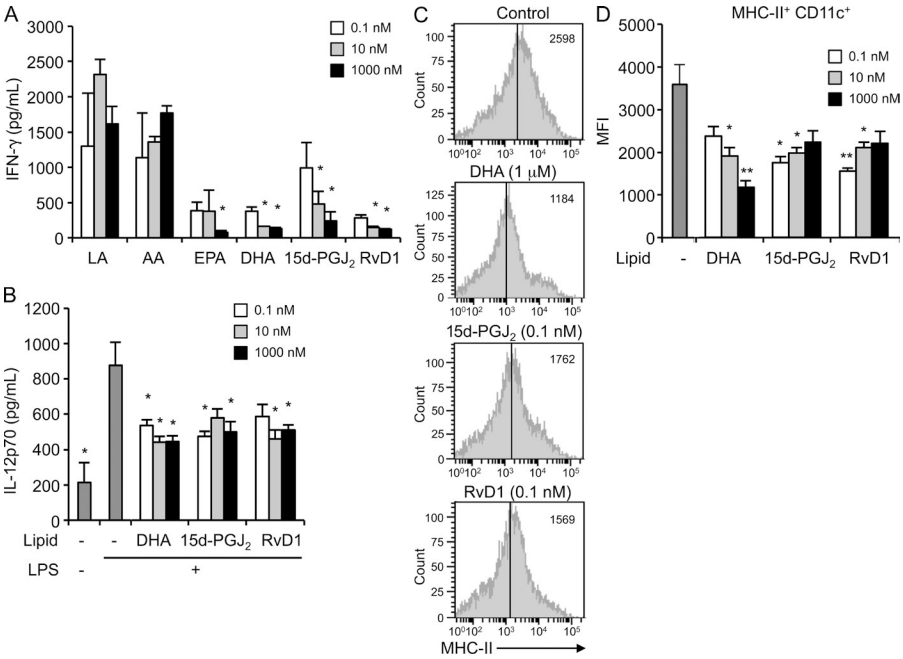

Figure 8. Effects of PUFAs and their metabolites on activation of LN cells and DCs. (A) LN cells obtained from DNFB-sensitized WT mice were stimulated with DNBS for 24 h in the presence of the indicated lipids to assess IFN-γ secretion (mean ± SEM, $n = 3$ per group; *, $P < 0.05$ versus the same concentration of LA). (B–D) BMDCs were stimulated with 10 ng/ml LPS in the presence or absence of the indicated concentrations of lipids for 24 h to assess the release of IL-12p70 by ELISA (mean ± SEM, $n = 4$ per group; *, $P < 0.05$ versus plus LPS without lipids; B) and the surface expression of MHC class II by flow cytometry (C and D). Representative FACS profiles with median fluorescence intensity (MFI) are indicated (C). Average scores of the MFI are evaluated (mean ± SEM, $n = 4$ per group; *, $P < 0.05$ and **, $P < 0.01$ versus without lipids; D). Results are representative of two (A) or three (B–D) independent experiments.

Published May 20, 2013

Nakano et al., 2009). Among the lymphoid-resident DC subsets, CD8α$^+$ DCs are responsible for cell-mediated immune responses, whereas CD4$^+$ DCs regulate humoral responses (Maldonado-López et al., 1999; Pulendran et al., 1999; den Haan et al., 2000; Pooley et al., 2001). PLA2G2D is preferentially expressed in lymphoid tissue-resident CD4$^+$CD11b$^+$ DCs as well as in dermal DCs, monocyte-derived inflammatory DCs/macrophages, and ex vivo-derived, GM-CSF-driven BMDCs.

Although PLA2G2D is largely dispensable for normal development of DCs as well as lymphocytes and other myeloid cells, its deficiency impairs resolution, rather than progression, of CHS with over-production of proinflammatory markers, while holding antiinflammatory markers unchanged, in both skin and regional LNs. Robust elevation of DC/macrophage surface markers and proinflammatory cytokines/chemokines in hapten-challenged *Pla2g2d*$^{-/-}$ mice over WT mice in the late phase of CHS indicates that PLA2G2D deficiency perturbs the termination program for the recruitment and activation of monocyte-derived inflammatory DCs/macrophages. In support of this, GM-CSF-driven BMDCs from *Pla2g2d*$^{-/-}$ mice have elevated expression of cell activation markers and can elicit skin inflammation after transferred into mice. The decrease of PLA2G2D expression in activated DCs also accords with the antiinflammatory property of this enzyme. In addition, a modestly increased splenic CD4$^+$ T cells in *Pla2g2d*$^{-/-}$ mice under normal condition might result from the increased activation of CD4$^+$ DCs.

During the process of inflammation, lipid mediator profiles switch from proinflammatory to antiinflammatory products, which in turn contribute to sequestration of the recruitment of inflammatory cells to the site (Levy et al., 2001; Serhan et al., 2008). Of importance, lipidomics profiling has delineated a critical role of PLA2G2D in the supply of a pool of free PUFAs that can be selectively linked to an array of pro-resolving lipid products in the skin-draining LNs. Thus, several DHA- and EPA-oxygenated products and AA-derived 15d-PGJ$_2$ were significantly reduced in the LNs by PLA2G2D deletion. The LN levels of free AA, EPA, and DHA were lower in *Pla2g2d*$^{-/-}$ mice even under noninflamed conditions, suggesting that PLA2G2D participates in the steady-state supply of a particular PUFA pool within the LNs. In contrast, Th1-promoting AA-derived mediators appear to be mostly derived from the PLA2G2D-independent AA pool, thus revealing an unexplored compartmentalization of distinct PUFA pools toward pro- versus antiinflammatory pathways. Although the molecular basis for the distinct compartmentalization of the pro- and antiinflammatory lipid pathways in the LNs is unclear at present, it may rely on when and where PLA2G2D secreted from DCs could encounter its target phospholipids during the process of immune response. The differential expression of downstream biosynthetic enzymes, each of which may be localized in distinct cell populations, could provide partly an explanation for the different coupling of PLA2G2D with pro- versus antiinflammatory lipid mediators. The preferred target phospholipids of PLA2G2D are particular PE molecular species with PUFAs such as DHA and AA. Considering that PE usually resides in the inner leaflet of the plasma membrane in resting cells, PLA2G2D might act on these PE species exposed on activated cells by a process of flip-flop or those released extracellularly from the cells (e.g., exosomes or microvesicles). Supporting the latter possibility, sPLA$_2$ acts on microvesicles shed from cells at inflamed sites (Fourcade et al., 1995) and leukocyte-derived microvesicles, which are temporally generated in inflammatory exudates during resolution, contain esterified biosynthetic precursors of pro-resolving mediators (Norling et al., 2011).

Collectively, we conclude that PLA2G2D is preferentially coupled with the biosynthesis of pro-resolving lipid mediators that could resolve LN inflammation. Our results are compatible with a recent report showing that mouse lymphoid tissues produce RvD1, which can regulate antibody production (Ramon et al., 2012). Also, free PUFAs by themselves might be protective against inflammation through acting on PUFA-sensing receptors (Diep et al., 2000; Oh et al., 2010) or through reducing the stress response (Ariyama et al., 2010). As such, the lack of PLA2G2D, and accordingly the decrease of the pro-resolving lipid mediators driven by this enzyme, may tip the balance toward a more aggressive inflammatory response in the LNs and thereby in the skin. The lipid-mobilizing role of PLA2G2D in local skin microenvironments remains to be elucidated.

PLA2G5 is expressed in macrophages and DCs (Giannattasio et al., 2010; Satake et al., 2004), and we have shown here that it is preferentially localized in CD11b$^+$CD11c$^-$ splenic macrophages. The expression of PLA2G2D in lymphoid organs and in CD11c$^+$ cells is much higher than that of PLA2G5 and other sPLA$_2$ isoforms. Beyond their distinct expression patterns, these two sPLA$_2$s afford opposite effects on DC functions and immunity; PLA2G5 facilitates antigen capture and presentation by DCs toward airway inflammation (Giannattasio et al., 2010), while PLA2G2D has pro-resolving roles in CHS (as shown in this study by gene targeting) and in experimental multiple sclerosis and colitis (as shown by injection of PLA2G2D-Fc fusion protein; von Allmen et al., 2009). Although the mechanism underlying the functional difference between these two sPLA$_2$s is unclear, it might rely at least partly on their distinct expression levels and on their different substrate selectivity in that PLA2G2D prefers PE bearing PUFAs (this study), whereas PLA2G5 prefers PE and PC bearing fatty acids with low degree of unsaturation (Chen and Dennis, 1998; Mitsuishi et al., 2007). Non-redundant roles of multiple sPLA$_2$s in a given process have also been documented for arthritis (offensive PLA2G2A versus defensive PLA2G5; Boilard et al., 2010) and for male reproduction (PLA2G3 for sperm maturation versus PLA2G10 for sperm activation; Escoffier et al., 2010; Sato et al., 2010). The contrasting roles of PLA2G2D versus PLA2G5 in the DC-related immunity represent another example of these occasions. Thus, individual sPLA$_2$s, which exhibit distinct substrate preferences or cellular locations in a given tissue or cell type, act spatiotemporally on different membrane targets, thereby linking to distinct biological outcomes. Although pan-sPLA$_2$

Downloaded from jem.rupress.org on August 18, 2013

Published May 20, 2013

inhibitors, which block classical $sPLA_2$s broadly, attenuate several disease models (Rosenson et al., 2009), dampening offensive and defensive $sPLA_2$s altogether might limit their therapeutic use (Bowton et al., 2005; Bradley et al., 2005). Our results point to an alternative strategy to use PLA2G2D, a resolving $sPLA_2$, for treatment of human disorders.

MATERIALS AND METHODS

Targeted disruption of the *Pla2g2d* gene. The *Pla2g2d*-targeting vector was constructed with a neomycin resistance (*Neo*^{r}) gene that was inserted between exons 1 and 2 of the *Pla2g2d* gene. ES cell transfection and embryo injections were performed by the Transgenic Resources Program (Department of Comparative Medicine, University of Washington, Seattle, WA). ES clones with homologous recombination were screened by PCR and Southern blotting. After germline transmission, *Pla2g2d*$^{+/-}$ mice were bred with C57BL/6NCrSLc (Japan SLC) mice ($n > 12$). Genotyping was performed on genomic DNA from tail biopsies by PCR using the primer pairs 5′-CCATCTGAACTTGAGTGGGAAGTGCCA-3′ and 5′-GCCTATGGGTCCCTCATGAG-3′ (Sigma Genosys), which amplified a 490-bp fragment specific for the WT allele, and 5′-GTGCTGTCAGAAGCATGATTGTT-3′ and 5′-GCCTATGGGTCCCTCATGAG-3′, which amplified a 530-bp fragment specific for the mutant allele. The reaction was 95°C for 10 s and then 35 cycles of 95°C for 0 s and 65°C for 1 min on Applied Biosystems 9800 Fast Thermal Cycler (Applied Biosystems). The PCR products were analyzed by 1.5% (wt/vol) agarose gel electrophoresis with ethidium bromide. All mice were housed in climate-controlled (23°C) specific pathogen–free facilities with a 12-h light-dark cycle, with free access to standard laboratory food (CE2; Laboratory Diet; CLEA Japan) and water. All procedures involving animals were performed in accordance with protocols approved by the Institutional Animal Care and Use Committees of the Tokyo Metropolitan Institute of Medical Science, Showa University, and the University of Washington.

Hapten-induced CHS. On day −5, mice (7–12-wk-old, male) were sensitized with 50 µl of 0.5% (vol/vol) DNFB in acetone/olive oil (4/1, vol/vol) on shaved abdominal skin. On day 0, ears were challenged by 20 µl of 0.3% DNFB to their dorsal and ventral surfaces. Ear thickness was measured for each mouse before and after elicitation for various time periods at a predetermined site with a micrometer, and the difference is expressed as ear swelling.

Quantitative RT-PCR. Total RNA was extracted from tissues and cells using TRIzol reagent (Invitrogen). First-strand cDNA synthesis was performed using a High Capacity cDNA Reverse transcription kit (Applied Biosystems). PCR reactions were performed using Power SYBR Green PCR system (Applied Biosystems) or TaqMan Gene Expression System (Applied Biosystems) on the ABI7700 Quantitative PCR system (Applied Biosystems). The probe/primer sets used were listed in Table S3.

Immunohistochemistry. Paraffin-embedded tissue sections (~4–7 µm thick) were incubated with Target Retrieval Solution (Dako), and then with rabbit anti–mouse or human PLA2G2D antibody, which did not cross-react with other $sPLA_2$s (Degousee et al., 2002), or control antibody at 1:2,000 dilution in 10 mM Tris-HCl (pH 7.4) containing 0.15 M NaCl and 0.1% BSA (TBS-BSA) overnight at 4°C. The sections were then treated with an EnVision+ System Staining kit (Dako) with diaminobenzidine substrate, followed by counterstaining with hematoxylin (Murakami et al., 2005; Sato et al., 2010). Human LN sections were obtained by surgery at Toho University Ohmori Hospital (Tokyo, Japan) after approval by the ethical committee of the faculty and informed consents from patients.

Confocal laser microscopy. Mouse frozen tissues mounted in OCT compound (Sakura Finetek) were cut into 20-µm thick sections using a cryomicrotome (CM3050S; Leica). The sections were incubated with 1.5 x Block Ace (DS Pharma Biomedical) in TBS for 30 min, and then with rabbit anti–mouse PLA2G2D antibody, phycoerythrin-conjugated hamster anti–mouse CD11c antibody (N418; eBioscience), or FITC-labeled rat anti–mouse F4/80 antibody (BM8; BioLegend) in TBS-BSA overnight at 4°C. For human tissues, rabbit anti–human PLA2G2D antibody and Alexa Fluor 488–labeled mouse anti–human CD11c antibody (3.9; BioLegend) were used. The sections were then treated with 1 µg/ml Alexa Fluor 647–labeled goat anti–rabbit IgG (Invitrogen) in TBS-BSA for 1 h, mounted in a VectaShield mounting medium (Vector laboratories), and analyzed with a confocal laser scanning microscope (LSM510 META; Carl Zeiss).

Flow cytometry. Mouse spleens or inguinal LNs were excised, minced in Hanks' solution (Nissui Pharmaceutical) with 2% (vol/vol) heat-inactivated FBS (Invitrogen) and 0.05% (wt/vol) sodium azide (Nacalai Tesque), and incubated with 400 U/ml collagenase type II (Worthington) with shaking for 30 min at 37°C. After adding 10 mM EDTA, the suspensions were passed through Cell Strainer 70-µm Nylon (Falcon; BD), and then centrifuged at 300 *g* for 5 min at 4°C. Splenocytes were treated for 2 min on ice with 10 mM Tris-HCl (pH 8.0) containing 0.84% (wt/vol) ammonium chloride to lyse red blood cells, centrifuged, and suspended in Hanks' solution. For AutoMACS analysis, the cells were resuspended at 10^7 cells/ml in AutoMACS buffer (PBS, 0.5% [wt/vol] BSA, and 2 mM EDTA), blocked with 0.5 µg/ml rat anti–mouse CD16/CD32 antibody (mouse BD Tc Block; BD) for 5 min at 4°C, and were added with 1/4 volume of appropriate MicroBeads (Miltenyi Biotec). After incubation for 15 min at 4°C, cells (~10^8 cells/500 µl) were resuspended in AutoMACS buffer and applied to AutoMACS Pro Separator (Miltenyi Biotec). For flow cytometry, the cells were blocked with mouse BD Tc Block, incubated with marker antibodies (listed in Table S4), and analyzed with a FACSAria III (BD) and FlowJo (Tree Star) software.

Culture of LN cells. LN cells (10^6 cells/ml) were isolated from mice that had been sensitized with DNFB for 5 d and cultured with or without 100 µg/ml DNBS (Alfa Aesar) in culture medium (RPMI 1640 containing 10% heat-inactivated FBS, 50 µM 2-ME, 2 mM L-glutamine, 25 mM Hepes, 1 mM nonessential amino acids, 1 mM sodium pyruvate, 100 U/ml penicillin, and 100 µg/ml streptomycin). After appropriate periods, RNA was extracted from the cells and subjected to quantitative RT-PCR, and the supernatants were subjected to ELISA for cytokines (eBioscience). As required for experiments, PUFAs, 15d-PGJ_2, and RvD1 (Cayman Chemicals) were added to the culture.

Culture of BMDCs and BMDMs. BM cells were cultured with mouse GM-CSF (10 ng/ml; PeproTech) for 9 d and with mouse M-CSF (100 ng/ml; Kyowa Kirin) for 3 d to obtain BMDCs and BMDMs, respectively (Lutz et al., 1999). The cells (2×10^6 cells/ml) were stimulated with LPS (Sigma-Aldrich) for 24 h to assess *Pla2g2d* expression by quantitative RT-PCR, cytokine release by ELISA, or surface expression of DC activation markers by FACS. For transfer of BMDCs into mice, the cells (2×10^6 cells/ml) were treated with 100 µg/ml DNBS for 24 h, resuspended in PBS at 10^6 cells/200 µl, and injected intravenously into recipient mice. After 5 d, the ears were challenged with 40 µl of 0.3% DNFB to monitor ear swelling.

Immunoblotting. Spleen (10 mg) was homogenized in 100 µl of 20 mM Tris-HCl (pH7.5) with a Polytron homogenizer. Protein concentrations were determined with a BCA protein assay kit (Thermo Fisher Scientific). The homogenates (10 µg protein) were subjected to SDS-PAGE on 15% (wt/vol) gels under nonreducing conditions and were electroblotted onto PVDF membranes (Bio-Rad Laboratories) with a semi-dry blotter (Transblot SD; Bio-Rad Laboratories). The membranes were blocked with 5% (wt/vol) skim milk in PBS containing 0.05% (vol/vol) Tween 20 (PBS-T), probed with goat anti-PLA2G2D antibody (sc-104297; Santa Cruz Biotechnology, Inc.) at 1:5,000 dilution in PBS-T for 2 h, incubated with horseradish peroxidase–conjugated anti-goat IgG (Zymed) at 1:5,000 dilution in PBS-T for 2 h, and then visualized by ECL Prime Western blotting detection reagent (GE Healthcare) with LAS-4000 (Fuji Film).

Downloaded from jem.rupress.org on August 18, 2013

ESI-MS. Tissues were soaked in 10 vol of methanol and homogenized with a Polytron homogenizer. After overnight incubation at −20°C, water was added to the mixture to give a final methanol concentration of 10% (vol/vol). As internal standards, 1 ng of *d4*-labeled leukotriene B_4, *d4*-labeled PGD_2, and *d8*-labeled 15-HETE (Cayman Chemicals) were added to the samples. The samples in 10% methanol were applied to Sep-Pak C18 cartridges (Waters), washed with 10 ml of hexane, eluted with 3 ml of methyl formate, dried up under N_2 gas, and solved in 60% methanol. The analysis of PUFAs and their metabolites was performed using a 4000Q-TRAP quadrupole-linear ion trap hybrid mass spectrometer (AB Sciex) with liquid chromatography (LC; LC-20AP; Shimazu) combined with an HTC PAL autosampler (CTC Analytics). The sample was applied to the Develosil C30-UG column (1 × 150 mm i.d., 3 µm particle; Nomura Chemical) coupled for ESI-MS/MS. The samples injected by an autosampler (10 µl) were separated by a step gradient with mobile phase A (water containing 0.1% acetic acid) and mobile phase B (acetonitrile: methanol = 4: 1; vol/vol) at a flow rate of 50 µl/min at 45°C. The detection of each lipid was performed by multiple reaction monitoring (Yamamoto et al., 2011).

PLA_2 reaction. Lipids were extracted from mouse LNs by the method of Bligh and Dyer (Bligh and Dyer, 1959). The LN membrane mimic composed of the tissue-extracted lipids (250 µg) was sonicated for 5 min in 100 mM Tris-HCl (pH 7.4) containing 4 mM $CaCl_2$ and then incubated for 1 h at 37°C with 200 nM recombinant mouse PLA2G2D (Rouault et al., 2007). After incubation, the lipids were mixed with internal standards (250 pmol of PE or PC with 14:0-14:0), extracted, and subjected to ESI-MS for detections of fatty acids, phospholipids, and lysophospholipids (Sato et al., 2010; Yamamoto et al., 2011).

Statistical analysis. Data are presented as the mean ± SEM. Statistical significance was evaluated by two-tailed Student's *t* test and Dunnett test at a significance level of $P < 0.05$.

Online supplemental material. Fig. S1 shows flow cytometry of splenocytes used in Fig. 1 D. Tables S1 and S2 show serum parameters and circulating blood cells in *Pla2g2d*$^{-/-}$ and *Pla2g2d*$^{+/+}$ mice under normal conditions. Table S3 is a list of primers used in quantitative RT-PCR. Table S4 is a list of antibodies used in flow cytometry. Online supplemental material is available at http://www.jem.org/cgi/content/full/jem.20121887/DC1.

We would like to thank Dr. Takehiko Yokomizo (Juntendo University, Tokyo, Japan) for technical assistance.

This work was supported by grants in aid for Scientific Research from the Ministry of Education, Culture, Sports, Science and Technology of Japan 22116005, 24390021 (to M. Murakami), 24890296 (to Y. Miki), 23591665 (to K. Yamamoto), 23790119 (to Y. Taketomi), and 23790120 (to H. Sato), Promoting Individual Research to Nurture the Seeds of Future Innovation and Organizing Unique Innovative Network (PRESTO) of Japan Science and Technology Agency (JST; to M. Murakami), and the Uehara, Mitsubishi, Terumo, and Toray Science Foundations (to M. Murakami).

The authors have no conflicting financial interests.

Submitted: 21 August 2012
Accepted: 29 April 2013

REFERENCES

Allenspach, E.J., M.P. Lemos, P.M. Porrett, L.A. Turka, and T.M. Laufer. 2008. Migratory and lymphoid-resident dendritic cells cooperate to efficiently prime naive CD4 T cells. *Immunity*. 29:795–806. http://dx.doi.org/10.1016/j.immuni.2008.08.013

Ariyama, H., N. Kono, S. Matsuda, T. Inoue, and H. Arai. 2010. Decrease in membrane phospholipid unsaturation induces unfolded protein response. *J. Biol. Chem.* 285:22027–22035. http://dx.doi.org/10.1074/jbc.M110.126870

Balestrieri, B., A. Maekawa, W. Xing, M.H. Gelb, H.R. Katz, and J.P. Arm. 2009. Group V secretory phospholipase A_2 modulates phagosome maturation and regulates the innate immune response against *Candida albicans*. *J. Immunol.* 182:4891–4898. http://dx.doi.org/10.4049/jimmunol.0803776

Bligh, E.G., and W.J. Dyer. 1959. A rapid method of total lipid extraction and purification. *Can. J. Biochem. Physiol.* 37:911–917. http://dx.doi.org/10.1139/o59-099

Boilard, E., Y. Lai, K. Larabee, B. Balestrieri, F. Ghomashchi, D. Fujioka, R. Gobezie, J.S. Coblyn, M.E. Weinblatt, E.M. Massarotti, et al. 2010. A novel anti-inflammatory role for secretory phospholipase A_2 in immune complex-mediated arthritis. *EMBO Mol. Med.* 2:172–187. http://dx.doi.org/10.1002/emmm.201000072

Bonventre, J.V., Z. Huang, M.R. Taheri, E. O'Leary, E. Li, M.A. Moskowitz, and A. Sapirstein. 1997. Reduced fertility and postischaemic brain injury in mice deficient in cytosolic phospholipase A_2. *Nature*. 390:622–625. http://dx.doi.org/10.1038/37635

Bostrom, M.A., B.B. Boyanovsky, C.T. Jordan, M.P. Wadsworth, D.J. Taatjes, F.C. de Beer, and N.R. Webb. 2007. Group V secretory phospholipase A_2 promotes atherosclerosis: evidence from genetically altered mice. *Arterioscler. Thromb. Vasc. Biol.* 27:600–606. http://dx.doi.org/10.1161/01.ATV.0000257133.60884.44

Bowton, D.L., A.A. Dmitrienko, E. Israel, B.G. Zeiher, and G.D. Sides. 2005. Impact of a soluble phospholipase A_2 inhibitor on inhaled allergen challenge in subjects with asthma. *J. Asthma*. 42:65–71. http://dx.doi.org/10.1081/JAS-200044748

Bradley, J.D., A.A. Dmitrienko, A.J. Kivitz, O.S. Gluck, A.L. Weaver, C. Wiesenhutter, S.L. Myers, and G.D. Sides. 2005. A randomized, double-blinded, placebo-controlled clinical trial of LY333013, a selective inhibitor of group II secretory phospholipase A_2, in the treatment of rheumatoid arthritis. *J. Rheumatol.* 32:417–423.

Byrum, R.S., J.L. Goulet, J.N. Snouwaert, R.J. Griffiths, and B.H. Koller. 1999. Determination of the contribution of cysteinyl leukotrienes and leukotriene B_4 in acute inflammatory responses using 5-lipoxygenase- and leukotriene A_4 hydrolase-deficient mice. *J. Immunol.* 163:6810–6819. http://www.jimmunol.org/content/163/12/6810

Chen, Y., and E.A. Dennis. 1998. Expression and characterization of human group V phospholipase A_2. *Biochim. Biophys. Acta*. 1394:57–64. http://dx.doi.org/10.1016/S0005-2760(98)00098-8

Curfs, D.M., S.A. Ghesquiere, M.N. Vergouwe, I. van der Made, M.J. Gijbels, D.R. Greaves, J.S. Verbeek, M.H. Hofker, and M.P. de Winther. 2008. Macrophage secretory phospholipase A_2 group X enhances anti-inflammatory responses, promotes lipid accumulation, and contributes to aberrant lung pathology. *J. Biol. Chem.* 283:21640–21648. http://dx.doi.org/10.1074/jbc.M710584200

Danno, K., K. Ikai, and S. Imamura. 1993. Anti-inflammatory effects of eicosapentaenoic acid on experimental skin inflammation models. *Arch. Dermatol. Res.* 285:432–435. http://dx.doi.org/10.1007/BF00372139

Degousee, N., F. Ghomashchi, E. Stefanski, A. Singer, B.P. Smart, N. Borregaard, R. Reithmeier, T.F. Lindsay, C. Lichtenberger, W. Reinisch, et al. 2002. Groups IV, V, and X phospholipases A_2s in human neutrophils: role in eicosanoid production and gram-negative bacterial phospholipid hydrolysis. *J. Biol. Chem.* 277:5061–5073. http://dx.doi.org/10.1074/jbc.M109083200

den Haan, J.M., S.M. Lehar, and M.J. Bevan. 2000. CD8(+) but not CD8(−) dendritic cells cross-prime cytotoxic T cells in vivo. *J. Exp. Med.* 192:1685–1696. http://dx.doi.org/10.1084/jem.192.12.1685

Diep, Q.N., R.M. Touyz, and E.L. Schiffrin. 2000. Docosahexaenoic acid, a peroxisome proliferator-activated receptor-α ligand, induces apoptosis in vascular smooth muscle cells by stimulation of p38 mitogen-activated protein kinase. *Hypertension*. 36:851–855. http://dx.doi.org/10.1161/01.HYP.36.5.851

Draper, E., C.M. Reynolds, M. Canavan, K.H. Mills, C.E. Loscher, and H.M. Roche. 2011. Omega-3 fatty acids attenuate dendritic cell function via NF-κB independent of PPARγ. *J. Nutr. Biochem.* 22:784–790. http://dx.doi.org/10.1016/j.jnutbio.2010.06.009

Escoffier, J., I. Jemel, A. Tanemoto, Y. Taketomi, C. Payre, C. Coatrieux, H. Sato, K. Yamamoto, S. Masuda, K. Pernet-Gallay, et al. 2010. Group X phospholipase A_2 is released during sperm acrosome reaction and controls fertility outcome in mice. *J. Clin. Invest.* 120:1415–1428. http://dx.doi.org/10.1172/JCI40494

Downloaded from jem.rupress.org on August 18, 2013

Published May 20, 2013

Fickenscher, H., S. Hör, H. Küpers, A. Knappe, S. Wittmann, and H. Sticht. 2002. The interleukin-10 family of cytokines. *Trends Immunol.* 23:89–96. http://dx.doi.org/10.1016/S1471-4906(01)02149-4

Fourcade, O., M.F. Simon, C. Viodé, N. Rugani, F. Leballe, A. Ragab, B. Fournié, L. Sarda, and H. Chap. 1995. Secretory phospholipase A_2 generates the novel lipid mediator lysophosphatidic acid in membrane microvesicles shed from activated cells. *Cell.* 80:919–927. http://dx.doi.org/10.1016/0092-8674(95)90295-3

Fujioka, D., Y. Saito, T. Kobayashi, T. Yano, H. Tezuka, Y. Ishimoto, N. Suzuki, Y. Yokota, T. Nakamura, J.E. Obata, et al. 2008. Reduction in myocardial ischemia/reperfusion injury in group X secretory phospholipase A_2-deficient mice. *Circulation.* 117:2977–2985. http://dx.doi.org/10.1161/CIRCULATIONAHA.107.743997

Giannattasio, G., D. Fujioka, W. Xing, H.R. Katz, J.A. Boyce, and B. Balestrieri. 2010. Group V secretory phospholipase A_2 reveals its role in house dust mite-induced allergic pulmonary inflammation by regulation of dendritic cell function. *J. Immunol.* 185:4430–4438. http://dx.doi.org/10.4049/jimmunol.1001384

Gomez, P.F., M.H. Pillinger, M. Attur, N. Marjanovic, M. Dave, J. Park, C.O. Bingham III, H. Al-Mussawir, and S.B. Abramson. 2005. Resolution of inflammation: prostaglandin E_2 dissociates nuclear trafficking of individual NF-κB subunits (p65, p50) in stimulated rheumatoid synovial fibroblasts. *J. Immunol.* 175:6924–6930. http://www.jimmunol.org/content/175/10/6924

Groeger, A.L., C. Cipollina, M.P. Cole, S.R. Woodcock, G. Bonacci, T.K. Rudolph, V. Rudolph, B.A. Freeman, and F.J. Schopfer. 2010. Cyclooxygenase-2 generates anti-inflammatory mediators from ω-3 fatty acids. *Nat. Chem. Biol.* 6:433–441. http://dx.doi.org/10.1038/nchembio.367

Heath, W.R., and F.R. Carbone. 2009. Dendritic cell subsets in primary and secondary T cell responses at body surfaces. *Nat. Immunol.* 10:1237–1244. http://dx.doi.org/10.1038/ni.1822

Henderson, W.R. Jr., E.Y. Chi, J.G. Bollinger, Y.T. Tien, X. Ye, L. Castelli, Y.P. Rubtsov, A.G. Singer, G.K. Chiang, T. Nevalainen, et al. 2007. Importance of group X-secreted phospholipase A_2 in allergen-induced airway inflammation and remodeling in a mouse asthma model. *J. Exp. Med.* 204:865–877. http://dx.doi.org/10.1084/jem.20070029

Honda, T., T. Matsuoka, M. Ueta, K. Kabashima, Y. Miyachi, and S. Narumiya. 2009. Prostaglandin $E_{(2)}$-$EP_{(3)}$ signaling suppresses skin inflammation in murine contact hypersensitivity. *J. Allergy Clin. Immunol.* 124:809–818: e2. http://dx.doi.org/10.1016/j.jaci.2009.04.029

Ishizaki, J., N. Suzuki, K. Higashino, Y. Yokota, T. Ono, K. Kawamoto, N. Fujii, H. Arita, and K. Hanasaki. 1999. Cloning and characterization of novel mouse and human secretory phospholipase $A_{(2)}$s. *J. Biol. Chem.* 274:24973–24979. http://dx.doi.org/10.1074/jbc.274.35.24973

Itano, A.A., S.J. McSorley, R.L. Reinhardt, B.D. Ehst, E. Ingulli, A.Y. Rudensky, and M.K. Jenkins. 2003. Distinct dendritic cell populations sequentially present antigen to CD4 T cells and stimulate different aspects of cell-mediated immunity. *Immunity.* 19:47–57. http://dx.doi.org/10.1016/S1074-7613(03)00175-4

Kabashima, K., D. Sakata, M. Nagamachi, Y. Miyachi, K. Inaba, and S. Narumiya. 2003. Prostaglandin E_2-EP4 signaling initiates skin immune responses by promoting migration and maturation of Langerhans cells. *Nat. Med.* 9:744–749. http://dx.doi.org/10.1038/nm872

Lambeau, G., and M.H. Gelb. 2008. Biochemistry and physiology of mammalian secreted phospholipases A_2. *Annu. Rev. Biochem.* 77:495–520. http://dx.doi.org/10.1146/annurev.biochem.76.062405.154007

Levy, B.D., C.B. Clish, B. Schmidt, K. Gronert, and C.N. Serhan. 2001. Lipid mediator class switching during acute inflammation: signals in resolution. *Nat. Immunol.* 2:612–619. http://dx.doi.org/10.1038/89759

Libby, P. 2002. Inflammation in atherosclerosis. *Nature.* 420:868–874. http://dx.doi.org/10.1038/nature01323

Lindbom, J., A.G. Ljungman, and C. Tagesson. 2005. Interferon γ-induced gene expression of the novel secretory phospholipase A_2 type IID in human monocyte-derived macrophages is inhibited by lipopolysaccharide. *Inflammation.* 29:108–117. http://dx.doi.org/10.1007/s10753-006-9007-x

Lu, B., C. Ebensperger, Z. Dembic, Y. Wang, M. Kvatyuk, T. Lu, R.L. Coffman, S. Pestka, and P.B. Rothman. 1998. Targeted disruption of the interferon-γ receptor 2 gene results in severe immune defects in mice. *Proc. Natl. Acad. Sci. USA.* 95:8233–8238. http://dx.doi.org/10.1073/pnas.95.14.8233

Lutz, M.B., N. Kukutsch, A.L. Ogilvie, S. Rössner, F. Koch, N. Romani, and G. Schuler. 1999. An advanced culture method for generating large quantities of highly pure dendritic cells from mouse bone marrow. *J. Immunol. Methods.* 223:77–92. http://dx.doi.org/10.1016/S0022-1759(98)00204-X

Maldonado-López, R., T. De Smedt, P. Michel, J. Godfroid, B. Pajak, C. Heirman, K. Thielemans, O. Leo, J. Urbain, and M. Moser. 1999. $CD8\alpha^+$ and $CD8\alpha^-$ subclasses of dendritic cells direct the development of distinct T helper cells in vivo. *J. Exp. Med.* 189:587–592. http://dx.doi.org/10.1084/jem.189.3.587

McGeachy, M.J. 2011. GM-CSF: the secret weapon in the $T_{(H)}17$ arsenal. *Nat. Immunol.* 12:521–522. http://dx.doi.org/10.1038/ni.2044

Mitsuishi, M., S. Masuda, I. Kudo, and M. Murakami. 2007. Human group III phospholipase A_2 suppresses adenovirus infection into host cells. Evidence that group III, V and X phospholipase A_2s act on distinct cellular phospholipid molecular species. *Biochim. Biophys. Acta.* 1771:1389–1396. http://dx.doi.org/10.1016/j.bbalip.2007.09.006

Moon, S.H., C.M. Jenkins, D.J. Mancuso, J. Turk, and R.W. Gross. 2008. Smooth muscle cell arachidonic acid release, migration, and proliferation are markedly attenuated in mice null for calcium-independent phospholipase $A_2\beta$. *J. Biol. Chem.* 283:33975–33987. http://dx.doi.org/10.1074/jbc.M805817200

Mukherjee, P.K., V.L. Marcheselli, C.N. Serhan, and N.G. Bazan. 2004. Neuroprotectin D1: a docosahexaenoic acid-derived docosatriene protects human retinal pigment epithelial cells from oxidative stress. *Proc. Natl. Acad. Sci. USA.* 101:8491–8496. http://dx.doi.org/10.1073/pnas.0402531101

Muñoz, N.M., A.Y. Meliton, J.P. Arm, J.V. Bonventre, W. Cho, and A.R. Leff. 2007. Deletion of secretory group V phospholipase A_2 attenuates cell migration and airway hyperresponsiveness in immunosensitized mice. *J. Immunol.* 179:4800–4807. http://www.jimmunol.org/content/179/7/4800

Murakami, M., R.S. Koduri, A. Enomoto, S. Shimbara, M. Seki, K. Yoshihara, A. Singer, E. Valentin, F. Ghomashchi, G. Lambeau, et al. 2001. Distinct arachidonate-releasing functions of mammalian secreted phospholipase A_2s in human embryonic kidney 293 and rat mastocytoma RBL-2H3 cells through heparan sulfate shuttling and external plasma membrane mechanisms. *J. Biol. Chem.* 276:10083–10096. http://dx.doi.org/10.1074/jbc.M007877200

Murakami, M., S. Masuda, K. Ueda-Semmyo, E. Yoda, H. Kuwata, Y. Takanezawa, J. Aoki, H. Arai, H. Sumimoto, Y. Ishikawa, et al. 2005. Group VIB Ca^{2+}-independent phospholipase $A_2\gamma$ promotes cellular membrane hydrolysis and prostaglandin production in a manner distinct from other intracellular phospholipases A_2. *J. Biol. Chem.* 280:14028–14041. http://dx.doi.org/10.1074/jbc.M413766200

Murakami, M., Y. Taketomi, C. Girard, K. Yamamoto, and G. Lambeau. 2010. Emerging roles of secreted phospholipase A_2 enzymes: Lessons from transgenic and knockout mice. *Biochimie.* 92:561–582. http://dx.doi.org/10.1016/j.biochi.2010.03.015

Murakami, M., Y. Taketomi, Y. Miki, H. Sato, T. Hirabayashi, and K. Yamamoto. 2011. Recent progress in phospholipase A_2 research: from cells to animals to humans. *Prog. Lipid Res.* 50:152–192. http://dx.doi.org/10.1016/j.plipres.2010.12.001

Nagamachi, M., D. Sakata, K. Kabashima, T. Furuyashiki, T. Murata, E. Segi-Nishida, K. Soontrapa, T. Matsuoka, Y. Miyachi, and S. Narumiya. 2007. Facilitation of Th1-mediated immune response by prostaglandin E receptor EP1. *J. Exp. Med.* 204:2865–2874. http://dx.doi.org/10.1084/jem.20070773

Nakajima, S., T. Honda, D. Sakata, G. Egawa, H. Tanizaki, A. Otsuka, C.S. Moniaga, T. Watanabe, Y. Miyachi, S. Narumiya, and K. Kabashima. 2010. Prostaglandin I_2-IP signaling promotes Th1 differentiation in a mouse model of contact hypersensitivity. *J. Immunol.* 184:5595–5603. http://dx.doi.org/10.4049/jimmunol.0903260

Nakano, H., K.L. Lin, M. Yanagita, C. Charbonneau, D.N. Cook, T. Kakiuchi, and M.D. Gunn. 2009. Blood-derived inflammatory dendritic cells in lymph nodes stimulate acute T helper type 1 immune responses. *Nat. Immunol.* 10:394–402. http://dx.doi.org/10.1038/ni.1707

Norling, L.V., M. Spite, R. Yang, R.J. Flower, M. Perretti, and C.N. Serhan. 2011. Cutting edge: Humanized nano-proresolving medicines mimic inflammation-resolution and enhance wound healing. *J. Immunol.* 186:5543–5547. http://dx.doi.org/10.4049/jimmunol.1003865

Downloaded from jem.rupress.org on August 18, 2013

Oh, D.Y., S. Talukdar, E.J. Bae, T. Imamura, H. Morinaga, W. Fan, P. Li, W.J. Lu, S.M. Watkins, and J.M. Olefsky. 2010. GPR120 is an ω-3 fatty acid receptor mediating potent anti-inflammatory and insulin-sensitizing effects. *Cell*. 142:687–698. http://dx.doi.org/10.1016/j.cell.2010.07.041

Ohtsuki, M., Y. Taketomi, S. Arata, S. Masuda, Y. Ishikawa, T. Ishii, Y. Takanezawa, J. Aoki, H. Arai, K. Yamamoto, et al. 2006. Transgenic expression of group V, but not group X, secreted phospholipase A_2 in mice leads to neonatal lethality because of lung dysfunction. *J. Biol. Chem*. 281:36420–36433. http://dx.doi.org/10.1074/jbc.M607975200

Pooley, J.L., W.R. Heath, and K. Shortman. 2001. Cutting edge: intravenous soluble antigen is presented to CD4 T cells by $CD8^-$ dendritic cells, but cross-presented to CD8 T cells by $CD8^+$ dendritic cells. *J. Immunol*. 166:5327–5330. http://www.jimmunol.org/content/166/9/5327

Pulendran, B., J.L. Smith, G. Caspary, K. Brasel, D. Pettit, E. Maraskovsky, and C.R. Maliszewski. 1999. Distinct dendritic cell subsets differentially regulate the class of immune response in vivo. *Proc. Natl. Acad. Sci. USA*. 96:1036–1041. http://dx.doi.org/10.1073/pnas.96.3.1036

Rajakariar, R., M. Hilliard, T. Lawrence, S. Trivedi, P. Colville-Nash, G. Bellingan, D. Fitzgerald, M.M. Yaqoob, and D.W. Gilroy. 2007. Hematopoietic prostaglandin D_2 synthase controls the onset and resolution of acute inflammation through PGD_2 and 15-deoxy$_{Delta12\ 14}$ PGJ_2. *Proc. Natl. Acad. Sci. USA*. 104:20979–20984. http://dx.doi.org/10.1073/pnas.0707394104

Ramon, S., F. Gao, C.N. Serhan, and R.P. Phipps. 2012. Specialized proresolving mediators enhance human B cell differentiation to antibody-secreting cells. *J. Immunol*. 189:1036–1042. http://dx.doi.org/10.4049/jimmunol.1103483

Rosenson, R.S., C. Hislop, D. McConnell, M. Elliott, Y. Stasiv, N. Wang, and D.D. Waters; PLASMA Investigators. 2009. Effects of 1-H-indole-3-glyoxamide (A-002) on concentration of secretory phospholipase A_2 (PLASMA study): a phase II double-blind, randomised, placebo-controlled trial. *Lancet*. 373:649–658. http://dx.doi.org/10.1016/S0140-6736(09)60403-7

Rossi, A., P. Kapahi, G. Natoli, T. Takahashi, Y. Chen, M. Karin, and M.G. Santoro. 2000. Anti-inflammatory cyclopentenone prostaglandins are direct inhibitors of IkappaB kinase. *Nature*. 403:103–108. http://dx.doi.org/10.1038/47520

Rouault, M., C. Le Calvez, E. Boilard, F. Surrel, A. Singer, F. Ghomashchi, S. Bezzine, S. Scarzello, J. Bollinger, M.H. Gelb, and G. Lambeau. 2007. Recombinant production and properties of binding of the full set of mouse secreted phospholipases A_2 to the mouse M-type receptor. *Biochemistry*. 46:1647–1662. http://dx.doi.org/10.1021/bi062119b

Samuelsson, B., S.E. Dahlén, J.A. Lindgren, C.A. Rouzer, and C.N. Serhan. 1987. Leukotrienes and lipoxins: structures, biosynthesis, and biological effects. *Science*. 237:1171–1176. http://dx.doi.org/10.1126/science.2820055

Satake, Y., B.L. Diaz, B. Balestrieri, B.K. Lam, Y. Kanaoka, M.J. Grusby, and J.P. Arm. 2004. Role of group V phospholipase A_2 in zymosan-induced eicosanoid generation and vascular permeability revealed by targeted gene disruption. *J. Biol. Chem*. 279:16488–16494. http://dx.doi.org/10.1074/jbc.M313748200

Sato, H., Y. Taketomi, Y. Isogai, Y. Miki, K. Yamamoto, S. Masuda, T. Hosono, S. Arata, Y. Ishikawa, T. Ishii, et al. 2010. Group III secreted phospholipase A_2 regulates epididymal sperm maturation and fertility in mice. *J. Clin. Invest*. 120:1400–1414. http://dx.doi.org/10.1172/JCI40493

Serbina, N.V., T.P. Salazar-Mather, C.A. Biron, W.A. Kuziel, and E.G. Pamer. 2003. TNF/iNOS-producing dendritic cells mediate innate immune defense against bacterial infection. *Immunity*. 19:59–70. http://dx.doi.org/10.1016/S1074-7613(03)00171-7

Serhan, C.N. 2007. Resolution phase of inflammation: novel endogenous anti-inflammatory and proresolving lipid mediators and pathways. *Annu. Rev. Immunol*. 25:101–137. http://dx.doi.org/10.1146/annurev.immunol.25.022106.141647

Serhan, C.N., S. Hong, K. Gronert, S.P. Colgan, P.R. Devchand, G. Mirick, and R.L. Moussignac. 2002. Resolvins: a family of bioactive products of ω-3 fatty acid transformation circuits initiated by aspirin treatment that counter proinflammation signals. *J. Exp. Med*. 196:1025–1037. http://dx.doi.org/10.1084/jem.20020760

Serhan, C.N., N. Chiang, and T.E. Van Dyke. 2008. Resolving inflammation: dual anti-inflammatory and pro-resolution lipid mediators. *Nat. Rev. Immunol*. 8:349–361. http://dx.doi.org/10.1038/nri2294

Shakhov, A.N., A.V. Rubtsov, I.G. Lyakhov, A.V. Tumanov, and S.A. Nedospasov. 2000. SPLASH (PLA2IID), a novel member of phospholipase A_2 family, is associated with lymphotoxin deficiency. *Genes Immun*. 1:191–199. http://dx.doi.org/10.1038/sj.gene.6363659

Shevach, E.M. 2009. Mechanisms of $Foxp3^+$ T regulatory cell-mediated suppression. *Immunity*. 30:636–645. http://dx.doi.org/10.1016/j.immuni.2009.04.010

Straus, D.S., G. Pascual, M. Li, J.S. Welch, M. Ricote, C.H. Hsiang, L.L. Sengchanthalangsy, G. Ghosh, and C.K. Glass. 2000. 15-deoxy-$\delta^{12,14}$-prostaglandin J2 inhibits multiple steps in the NF-κ B signaling pathway. *Proc. Natl. Acad. Sci. USA*. 97:4844–4849. http://dx.doi.org/10.1073/pnas.97.9.4844

Suzuki, N., J. Ishizaki, Y. Yokota, K. Higashino, T. Ono, M. Ikeda, N. Fujii, K. Kawamoto, and K. Hanasaki. 2000. Structures, enzymatic properties, and expression of novel human and mouse secretory phospholipase $A_{(2)}$s. *J. Biol. Chem*. 275:5785–5793. http://dx.doi.org/10.1074/jbc.275.8.5785

Tamura, T., P. Tailor, K. Yamaoka, H.J. Kong, H. Tsujimura, J.J. O'Shea, H. Singh, and K. Ozato. 2005. IFN regulatory factor-4 and -8 govern dendritic cell subset development and their functional diversity. *J. Immunol*. 174:2573–2581. http://www.jimmunol.org/content/174/5/2573

Tomobe, Y.I., K. Morizawa, M. Tsuchida, H. Hibino, Y. Nakano, and Y. Tanaka. 2000. Dietary docosahexaenoic acid suppresses inflammation and immunoresponses in contact hypersensitivity reaction in mice. *Lipids*. 35:61–69. http://dx.doi.org/10.1007/s11745-000-0495-0

Trivedi, S.G., J. Newson, R. Rajakariar, T.S. Jacques, R. Hannon, Y. Kanaoka, N. Eguchi, P. Colville-Nash, and D.W. Gilroy. 2006. Essential role for hematopoietic prostaglandin D_2 synthase in the control of delayed type hypersensitivity. *Proc. Natl. Acad. Sci. USA*. 103:5179–5184. http://dx.doi.org/10.1073/pnas.0507175103

Uozumi, N., K. Kume, T. Nagase, N. Nakatani, S. Ishii, F. Tashiro, Y. Komagata, K. Maki, K. Ikuta, Y. Ouchi, et al. 1997. Role of cytosolic phospholipase A_2 in allergic response and parturition. *Nature*. 390:618–622. http://dx.doi.org/10.1038/37622

Valentin, E., R.S. Koduri, J.C. Scimeca, G. Carle, M.H. Gelb, M. Lazdunski, and G. Lambeau. 1999. Cloning and recombinant expression of a novel mouse-secreted phospholipase A_2. *J. Biol. Chem*. 274:19152–19160. http://dx.doi.org/10.1074/jbc.274.27.19152

Villadangos, J.A., and P. Schnorrer. 2007. Intrinsic and cooperative antigen-presenting functions of dendritic-cell subsets in vivo. *Nat. Rev. Immunol*. 7:543–555. http://dx.doi.org/10.1038/nri2103

von Allmen, C.E., N. Schmitz, M. Bauer, H.J. Hinton, M.O. Kurrer, R.B. Buser, M. Gwerder, S. Muntwiler, T. Sparwasser, R.R. Beerli, and M.F. Bachmann. 2009. Secretory phospholipase A_2-IID is an effector molecule of $CD4^+CD25^+$ regulatory T cells. *Proc. Natl. Acad. Sci. USA*. 106:11673–11678. http://dx.doi.org/10.1073/pnas.0812569106

Vremec, D., J. Pooley, H. Hochrein, L. Wu, and K. Shortman. 2000. CD4 and CD8 expression by dendritic cell subtypes in mouse thymus and spleen. *J. Immunol*. 164:2978–2986. http://www.jimmunol.org/content/164/6/2978

Weinrauch, Y., P. Elsbach, L.M. Madsen, A. Foreman, and J. Weiss. 1996. The potent anti-*Staphylococcus aureus* activity of a sterile rabbit inflammatory fluid is due to a 14-kD phospholipase A_2. *J. Clin. Invest*. 97:250–257. http://dx.doi.org/10.1172/JCI118399

Yamamoto, K., Y. Taketomi, Y. Isogai, Y. Miki, H. Sato, S. Masuda, Y. Nishito, K. Morioka, Y. Ishimoto, N. Suzuki, et al. 2011. Hair follicular expression and function of group X secreted phospholipase A_2 in mouse skin. *J. Biol. Chem*. 286:11616–11631. http://dx.doi.org/10.1074/jbc.M110.206714

Yao, C., D. Sakata, Y. Esaki, Y. Li, T. Matsuoka, K. Kuroiwa, Y. Sugimoto, and S. Narumiya. 2009. Prostaglandin E_2-EP4 signaling promotes immune inflammation through Th1 cell differentiation and Th17 cell expansion. *Nat. Med*. 15:633–640. http://dx.doi.org/10.1038/nm.1968

Yokoyama, M., H. Origasa, M. Matsuzaki, Y. Matsuzawa, Y. Saito, Y. Ishikawa, S. Oikawa, J. Sasaki, H. Hishida, H. Itakura, et al; Japan EPA lipid intervention study (JELIS) Investigators. 2007. Effects of eicosapentaenoic acid on major coronary events in hypercholesterolaemic patients (JELIS): a randomised open-label, blinded endpoint analysis. *Lancet*. 369:1090–1098. http://dx.doi.org/10.1016/S0140-6736(07)60527-3

Downloaded from jem.rupress.org on August 18, 2013

The Journal of Experimental Medicine

SUPPLEMENTAL MATERIAL

Mike et al., http://www.jem.org/cgi/content/full/jem.20121887/DC1

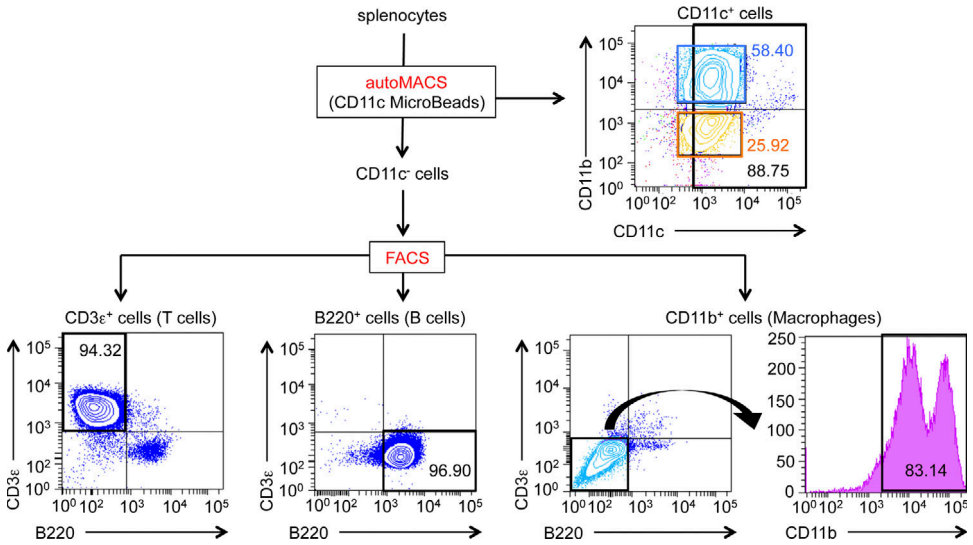

Figure S1. Flow cytometry of mouse splenocytes. Mouse splenocytes were separated into CD11c⁺ and CD11c⁻ populations by AutoMACS. CD11c⁻ cells were further sorted into CD3ε⁺ T cells, B220⁺ B cells, and CD11b⁺ macrophages. Purities of individual cell populations, which were used in Fig. 1 D, are indicated by boxes.

Table S1. Serum biochemical parameters in *Pla2g2d*$^{+/+}$ and *Pla2g2d*$^{-/-}$ mice under normal housing conditions

Parameters	Genotypes		Units
	Pla2g2d$^{+/+}$	*Pla2g2d*$^{-/-}$	
Alkaline phosphatase	135.3 ± 70.5	105.8 ± 41.2	U/liter
Alanine aminotransferase	30.9 ± 11.1	24.5 ± 3.1	U/liter
Bilirubin	0.3 ± 0.1	0.3 ± 0.1	mg/dl
Albumin	3.7 ± 0.5	3.6 ± 0.4	mg/dl
Nitrogen urea	28.5 ± 4.9	29.5 ± 11.5	mg/dl
Total cholesterol	77.4 ± 28.1	83.0 ± 11.5	mg/dl

Male 15-wk-old *Pla2g2d*$^{+/+}$ and *Pla2g2d*$^{-/-}$ mice were anesthetized and blood samples were collected by cardiac puncture. Sera were applied to a clinical chemistry analyzer VetScan with V-DPP rotors (n = 8). Data are pooled results from two experiments. None of these parameters differed significantly between the genotypes.

Table S2. Circulating blood cells in *Pla2g2d*$^{+/+}$ and *Pla2g2d*$^{-/-}$ mice under normal housing conditions

Cell populations	Genotypes		Units
	Pla2g2d$^{+/+}$	*Pla2g2d*$^{-/-}$	
Leukocytes	8.18 ± 1.11	7.89 ± 1.40	x 10^9 cells/liter
Lymphocytes	7.02 ± 1.04	6.47 ± 1.07	x 10^9 cells/liter
Granulocytes	0.76 ± 0.11	0.96 ± 0.29	x 10^9 cells/liter
Monocytes	0.39 ± 0.15	0.46 ± 0.18	x 10^9 cells/liter
Erythrocytes	9.97 ± 0.36	9.98 ± 0.13	x 10^{12} cells/liter
Platelets	0.59 ± 0.04	0.55 ± 0.04	x 10^{12} cells/liter

Blood samples of 15-wk-old male *Pla2g2d*$^{+/+}$ and *Pla2g2d*$^{-/-}$ mice were collected from tail biopsy with 10 mM EDTA as an anti-coagulant. The samples were applied to the clinical blood cell analyzer VetScan HM to determine the numbers of circulating blood cells (n = 9). Data are pooled results from two experiments. None of these parameters differed significantly between the genotypes.

Table S3. A list of primers used in quantitative RT-PCR

Gene	Accession number	Forward primer	Reverse primer	Probe number (Roche)
Ccl2	NM_011333.3	5′-CATCCACGTGTTGGCTCA-3′	5′-GATCATCTTGCTGGTGAATGAGT-3′	62
Ccr2	NM_009915.2	5′-ACCTGTAAATGCCATGCAAGT-3′	5′-TGTCTTCCATTTCCTTTGATTTG-3′	27
Cd11b	NM_001082960.1	5′-CAATAGCCAGCCTCAGTGC-3′	5′-GAGCCCAGGGGAGAAGTG-3′	76
Cd11c	NM_021334.2	5′-ATGGAGCCTCAAGACAGGAC-3′	5′-GGATCTGGGATGCTGAAATC-3′	20
Cd68	NM_009853.1	5′-GACCTACATCAGAGCCCGAGT-3′	5′-CGCCATGAATGTCCACTG-3′	96
Foxp3	NM_054039.1	5′-TCAGGAGCCCACCAGTACA-3′	5′-TCTGAAGGCAGAGTCAGGAGA-3′	78
Gapdhs	NM_008085.1	5′-CCTTGAGATCAACACGTACCAG-3′	5′-CGCCTGTACACTCCACCAC-3′	1
Ifng	NM_008337.1	5′-ATCTGGAGGAACTGGCAAAA-3′	5′-TTCAAGACTTCAAAGAGTCTGAGGTA-3′	21
Il1b	NM_008361.3	5′-TGTAATGAAAGACGGCACACC-3′	5′-TCTTCTTTGGGTATTGCTTGG-3′	78
Il6	NM_031168.1	5′-GCTACCAAACTGGATATAATCAGGA-3′	5′-CCAGGTAGCTATGGTACTCCAGAA-3′	6
Il10	NM_010548.1	5′-CAGAGCCACATGCTCCTAGA-3′	5′-TGTCCAGCTGGTCCTTTGTT-3′	41
Il12a	NM_008351.1	5′-ATCACAACCATCAGCAGATCA-3′	5′-CGCCATTATGATTCAGAGACTG-3′	49
Pla2g2d	NM_011109.1	5′-GCTCTGGGCTGGAACTATGA-3′	5′-CCTGGGTTGCAGTTATACCG-3′	66
Pla2g5	NM_011110.2	5′-CTCACACTGGCTTGGTTCCT-3′	5′-CATGGACTTGAGTTCTAGCAAGC-3′	95
S100a9	NM_009114.2	5′-CACCCTGAGCAAGAAGGAAT-3′	5′-TGTCATTTATGAGGGCTTCATTT-3′	31
Tgfb1	NM_011577.1	5′-TGGAGCAACATGTGGAACTC-3′	5′-CAGCAGCCGGTTACCAAG-3′	72
Tnf	NM_013693.1	5′-TCTTCTCATTCCTGCTTGTGG-3′	5′-GGTCTGGGCCATAGAACTGA-3′	49
Rn18s	-	5′-TCGAGGCCCTGTAATTGGAA-3′	5′-CCCTCCAATGGATCCTCGTT-3′	-
Pla2g1b		Taq man probe (Applied Biosystems) No. 00478249		
Pla2g2d		Taq man probe (Applied Biosystems) No. 00478250		
Pla2g2e		Taq man probe (Applied Biosystems) No. 00478870		
Pla2g2f		Taq man probe (Applied Biosystems) No. 00478872		
Pla2g5		Taq man probe (Applied Biosystems) No. 00448162		
Pla2g10		Taq man probe (Applied Biosystems) No. 00449532		

Table S4. A list of antibodies used in flow cytometry

Molecule	Clone	Ig subclass	Fluorescent labeling	Source
CD3ε	145-2C11	Hamster IgG	Alexa Fluor 488	BioLegend
			APC	eBioscience
			FITC	BioLegend
CD4	GK1.5	Rat IgG2b	phycoerythrin	BioLegend
CD8α	53-6.7	Rat IgG2a	Alexa Fluor 647	BioLegend
CD11b	M1/70	Rat IgG2b	FITC	BioLegend
			phycoerythrin	BioLegend
CD11c	N418	Hamster IgG	Alexa Fluor 700	BioLegend
			Biotin	BioLegend
			Pacific blue	BioLegend
			phycoerythrin	eBioscience
CD16/32	2.4G2	Rat IgG2b	-	BD
	93	Rat IgG2a	-	BioLegend
CD25	PC61	Rat IgG1	Alexa Fluor 488	BioLegend
CD44	IM7	Rat IgG2b	phycoerythrin	BD
CD45R/B220	RA3-6B2	Rat IgG2a	Alexa Fluor 647	BD
CD62L	MEL-14	Rat IgG2a	APC	BioLegend
CD80	16-10A1	Hamster IgG	APC	BioLegend
CD86	GL-1	Rat IgG2a	Biotin	BioLegend
FOXP3	FJK-16s	Rat IgG2a	Biotin	eBioscience
MHC class II	M5/114.15.2	Rat IgG2b	FITC	BioLegend
Streptavidin[a]	-	-	FITC	eBioscience
			PE/Cy7	BioLegend

[a]Used in combination with biotin-labeled antibodies.